**Master's Thesis**

# Biped Simulation of a Wheeled Flexible Robot

**Muhammad Talha Ilyas**

A thesis submitted for the award of the
degree of

**M.Sc. Mechatronics Engineering**

Submitted to

**Supervisor: Prof. Giovanni Gerardo Muscolo**


**Department of Electronics & Telecommunications**

**Politecnico di Torino**

**July 2019**

# ABSTRACT

The investigation of humanoid locomotion is an exceptional and dynamic region in the field of technology. Not only it provides the basic key for the humanoid robot to integrate in the human world but it also gives the possibility for the humans to better understand the human body and functioning of its compounding parts. Direct involvement of kinematics, dynamics and actuation as per the behavior delineated by human, make human like motion an intricate method. It is clear that human-friendly robots would be much more different than the today's industrial robots. Therefore, there is a need to continuously improve our models by exploiting the different areas of mechanical design and control of the robot to make them efficient, cheap and safe for the human environment.

This work presents the simulation of creative design, inspired by ROLLO robot (developed in BrainHuRo project), which focused on simplifying the biped humanoid locomotion in the domestic scenario. The idea is to maintain the flexibility and maneuverability of humanoid robot but at the same time should have less complexity and consume the suitable amount of energy with the lower impact on the environment. It is done by introducing wheels on the feet and replacing the rigid links in the legs with the flexible link. By exploiting the torsional and flexural behaviors of the flexible links, we can avoid the actuated joints and would have the passive joints. This would allow the robot to perform an alternating leg human like motion by using only two motors. There are 2 free wheels on each leg, which allows the robot to maintain the standing position without any actuation. Unconventional use of the cylindrical helical springs would improve the power consumption of the robot as well as they would pose much safer in the domestic environment.

The modelling and simulation of the ROLLO robot to create a dynamic simulation of the human like movement has been realized using 2 different software Solid works and MATLAB. The 3D-modelling of the Robot is done in solid works (except springs). The torsional and flexural behavior of the springs and the control of the ROLLO robot in the world environment was performed in MATLAB. The various level of controls has been utilized for the

stable movement. The tradeoff between balance, energy consumption and the oscillations have been performed in the different level of controls. The level of control is started from the evaluation of the smooth trajectory for the robot until the feedback position control for the oscillations using PID. The different results are obtained on 4 distinct velocities and 2 different configurations of the leg (one with 2 springs in each leg the other one is 3 springs in each leg) while performing the forward motion and rotation (clockwise anticlockwise) on the planar surface.

The major area of the research was to create a torsional and flexural behavior in MATLAB and to develop a control for human-like walking. This thesis is only the starting point of a broad spectrum of other possible future works: from the control structure completion and whole-body control application, to deep learning and reinforcement learning for human locomotion, from testing in the flat domestic environment and testing in the rough terrain with obstacle and certainly the transition from simulation to practice on the real platform such as ROLLO developed at BrainHuRo.

TABLE OF CONTENTS

# LIST OF FIGURES

# LIST OF TABLES

# ACKNOWLEDGMENTS

I have been lucky enough to receive huge amount of support from a lot of people, constantly throughout this time. Appreciation in the word might not be enough to express how thankful I am for their support.

For that, I would first like to thank my thesis advisor Prof G.G Muscolo of the Mechanical Department at Politecnico di Torino. His vast expertise in the field serve as a backbone for my research. I would also like to thank him specially for his availability and patience throughout this period

I would also like to thank experts who were involved in this research project indirectly as a mentor. Sebastian Castro and Swarooph Nirmal from MathWorks robotic arena, without there passionate participation and input, it would have been impossible to finish the research.

My parents and family deserves a special thanks, without their love, support and prayers nothing of this would be possible. To my partner, who stood by my side throughout this degree, whose continuous motivation and encouragement led me to work towards the betterment every single day. To my friends who always stood by myside through all the thick and thin.

*Chapter 1*

# Introduction

The brief overview of the problem and a novel approach to tackle that problem is presented in this chapter. An overall overview of the thesis is also presented in this thesis.

## 1.1 Statement of Problem

This work presents the design and development of a new-generation biped robot. Its modeling and simulation have been realized by using Solid works and MATLAB.

Recent advancement in technologies requires a faster, energy efficient and high-performance humanoid robot which can provide support to human activities and to help society which has depleting youth and increasing number of aging human population. Keeping the flexibility and maneuverability of humanoid robot but at the same time should have less complexity and consume the suitable amount of energy. The point which could not be neglected was the safety of the people sharing the environment with the robot.

The answer of the problem was provided in BrainHuRo project [3] by creating a robot able to provide biped motion on planar surface while transmitting the images to brain computer interface (BCI) technologies [5] which shows that image on tablet to the patients affected by amyotrophic lateral sclerosis (ALS) disease and cannot mobilize him/herself.

## 1.2 Novelty of this research

This research is based on the novel design proposed in the Brainhuro project [3]. In the paper, the innovative engineering design for humanoid robot was implemented by reducing the complexity maintaining the efficiency of the Robot and also to overcome the limits faced by humanoid in real world environment in terms of safety and robustness.

Area which is particularly focused here is the humanoid motion resemblance on planar surface in terms of its movement and shape, instead of exactly mimicking the human motion which consist of highly actuated DOFs. The Novel approach experimentally suggest that it is not necessary to have a complex structure with excessive number of DOFs, the same functions can be provided by comparatively less complex structure consisted of wheels and passive joints using springs in the leg links instead of rigid link. The created robot ROLLO efficiently saves the actuation amount whereas can maintain standing position without any actuation. Only two motors are used in the leg to drive the robot. The main characteristic was obtained by carefully designing the mechanical structure.

## 1.3 Thesis Overview

**Chapter 2 – Robotics and ROLLO**

This chapter provides an overview of some of the fundamental theory within the field of robotics. which will provide the reader with an introduction to the terminology and theory used throughout the thesis. A detailed concept, as well as an explanation to the reference work on which this thesis is based on is described. This chapter will also present an overview of the method used while developing ROLLO prototype. A declaration of what information the implementation is based on will be provided. A discussion of the implementation's limitations, assumptions and range of validity will be held.

**Chapter 3 - Implementation and Control**

This chapter aims to explain the implementation needed to complete the deliverables explained in Method. The chapter aims to provide a more detailed view of the work done during the thesis.

**Chapter 4 - Results and Discussion**

In this chapter all results will be presented and discussed. The tests are conducted according to the description in Method. The conclusions drawn from the results achieved during the thesis will be stated in this chapter.

*Chapter 2*

# Robotics and ROLLO

## 2.1 State of the art

Human like gait is the most desirable and a fancied concept in the field of Robotics due to its many benefits. Film, fantasy and entertainment promise us that humanoids will cook for us, dry for us, become our companions and educate our kids. Recently many humanoid robots are making their way to commercial market and gaining the spot light of media but these early generations of commercially available humanoids, like many new techniques, are expensive curiosities that help entertainment, but little else. Humanoid robots can already automatically decompose tasks required to execute high-level, complex orders by gesture and voice. Humanoids can adjust and organize current usefulness and create new practices utilizing a scope of Artificial intelligence strategies like machine learning. Humanoids can demonstrate the perfect development for robots to communicate with humans. All things considered, people will in general collaborate normally with other human elements; in our cerebrums, the interface is designed. Humanoid alludes to any being whose body structure takes after that of a human: head, legs, arms, hands. Be that as it may, it is likewise a robot made to look like a human both in appearance and conduct. In 1973, the development of the world's first humanoid robot was begun at the Waseda University in Tokyo under the bearing of Ichiro Kato. The primary full-scale human robot on the planet was called WABOT-1. After it, in 1980, at Waseda University was developed also WL-9DR, the world's first robot to exhibit quasi dynamic walking. Then, in 1985, with Hitachi Ltd. Was developed

WHL-11 (Waseda Hitachi Leg-11) biped, walking robot. Starting from then until today the robotics field is in constant development.

Robots can be built both for industrial and for research purposes. The differentiation is related to the fact that in one case, time, costs and robustness of the solution are considered as the main aspects in the development process, while the second one aims at building the most advanced and challenging solutions [70].

While focusing on the second aspect we can still see that the technological research even after an extensive work for years cannot be able to mimic the agility of infant child in the robots though many researchers have present different approaches to work towards the betterment of Biped Humanoid robots. [1] Research proposed and proved the effective formula to calculate ZMP value which are very much close to the projected or ideal value for the Humanoid robot locomotion. This technique determines the center of mass (COM) and used the force-torques values using the FT sensors present on the feet. It was tested on SABIAN robot in Italy. [29] The ZMP strength foundation expresses that the biped won't tumble down as long as the ZMP stays inside the convex hull of the foot-support. In these studies, the authors impose the motion of the lower limb kinematics from human kinematic data, which they term synergies. Along these lines, the ZMP model is utilized to switch between low-level controllers (which fulfill some target capacities like direction following) and perhaps maintain a strategic distance from obstacles. [12] Biped strolling can be characterized by the demonstrating of the predefined ZMP references to the conceivable body swings or CoM direction. [28] A mobile framework can understand a predefined development if and just if the related point extends vertically inside the raised body of the contact focuses. How about we consider then the flat revolution energy of gravity and "dynamic" powers around the

projection of the point called ZMP. The even pivot energy of contact powers is likewise equivalent to zero around this anticipated point, what could prompt call it additionally the Center of Pressure. "ZMP/CoP" criterion can't discriminate accurately situations where the framework is powerfully adjusted from situations where it's not in circumstances even as straightforward as climbing upstairs. [38] Paper proposes a strategy to decrease the movement scope of the trunk by producing an ideal direction of the ZMP. The direction is dictated by a fuzzy logic dependent on the leg directions that are subjectively chosen. The subsequent ZMP direction is like human's one and the ZMP ceaselessly pushes ahead. The proposed plan is simulated on a 7 DOF biped robot and the simulation results demonstrate that it doesn't require an enormous swing movement of the trunk and in this manner fundamentally balances out the biped robot. [8] Locomotion itself is the much harder problem as compare to the manipulator control, the most important state variables in the locomotion cannot be measured directly but through the indirect methods. One may think that the manipulation in terms of the task to be accomplished, then one is free to use whatever specialized control methods to produce the desired task. [4] ankle-foot, knee and Hip-pelvis joints present us the perspective of whole body performance and its energy constraints. To go through stance and swing phase effectively can be achieved by rigid flexible, flexible, actuated or non-actuated feet, quasi passive solution for knee are also present whereas the pelvis plays and important role in overall gait. Study also suggest to consider frontal and transversal frames rather than looking just on sagittal plane. [34] From the perspective of effectiveness in term of energy, ZMP and such strolling examples are not alluring since torque must be consistently applied to the knee joint to keep up a twisted knee pose as to maintain a strategic distance from inverse kinematics. [2] Whereas, one research proposes that changing the $K_a$ [environment stiffness matrix] values give the possibility to modify the

compliance of any external joints in robot. It was tested on DEXTER (a Humanoid arm with 8 DOF), increasing the value would give the arbitrary resistance to the arm and would cause the arm to stop at desired position. [3] Another idea exploits the torsional and flexural behavior of the spring in the humanoid legs instead of the actuated one. ROLLO robot used for BCI (brain computer interface) uses the wheeled legs with springs with the passive joints instead of actuated.

Human like complaint in the humanoid locomotion is composed of the many factors, one must see the important role of humanoid joint in the gait. [5] Brainhuro project *(Dec,2014-Dec,2016)* sheds a light on the energy consumption of the Humanoid robot SABIAN while performing the gait. The report separately mentioned the energy consumption of ankle, knee and hip pitch joints. [7] For two legged machine, walking is a natural dynamic, which, on the steady slope, can perform a human like gait without any need of control or an energy input. The traits of machine are easily demonstrated if it is controlled by only gravity, and can be combined with active energy to get the efficient result on the different kind of terrains. [9] Robot human like gait isn't an undeniable decision when both economy and flexibility are wanted, wheeled vehicles are competent on various trains and are about magnificent as far as economy. Legged locomotion appears energetically economical when they are equipped with either actuator similar to humans' or discontinuous nonlinear mechanism that can reduce energetic losses to support a load. This high versatility demands that ZMP remain applicable until the serious advancement is made in theoretical control approaches. [16] An extraordinary drew closer for the joint compliance is received in Lucy reenactment program, it is that the biped isn't actuated with the traditional electrical drives however with creased pneumatic artificial muscles. In an opposing arrangement of such muscles both

the torque and the compliance are controllable. In addition, they have the ability of engrossing shocks and store and discharge motion energy [17] Variable stiffness can improve the capacity of human-robot associating. In such manner adaptable rack and apparatus component is utilized which is the mix of a non-linear flexible component and a linear adjusting mechanism, giving advantage of conservativeness. The gear uprooting as for the adaptable gear rack is perpendicular to the joint stacking force so the power required for stiffness regulating is as low as 14.4 W, giving advantages of vitality sparing. [18] In robotics, Air Muscle is used as the analogy of the biological motor for locomotion or manipulation. It has favorable circumstances like the inactive Damping, great power-weight proportion and use in harsh conditions. Upon the increase in air pressure to muscle, it is observed that less pressure increase is needed initially to let Air Muscle contract. Furthermore, contraction of Air Muscle increases with the increase of the trapped volume. When the load is kept constant and pressure is increased, experiment exhibits the shortening behavior of Air muscle. Also, it contracts with decrement in loads and shortens to minimum length at the maximum volume trapped in it. [35] This paper explores a model of biped robot which utilizes least control and elastic passive joints roused from the structures of biological frameworks. The test results demonstrate that, with an appropriate leg structure of passive dynamics and elasticity, an attractor condition of human-like gait can be accomplished through very straightforward control without tangible input despite the fact that it was tested only in planar condition (i.e. yaw, pitch, and rotation movement are fixed). It would be particularly interesting to extend the same leg design for both walking and running behaviors. The transition between both gaits can also be investigated along the same line of research by using the proposed model.

[44] Classical and substantial controllers with high control gains are not fit to coordinate and work intimately with people. Besides, this actuation approach can weaken different qualities as for example energy efficiency. This feature is exploited using the dynamic property of energy storage in the flexible systems while stiff system cannot store energy. [43] Muscles and ligaments change their firmness as a component of the movement and task they need to perform. Arm muscles expect a solid arrangement when the arm needs to play out an exact assignment, while they are consistent when they are playing out the "loading" period of a throw. So also, in the event that we examine hopping we see that leg muscles are consistent during the "stacking" period of the hop or during the landing stage where they ingest the shocks, while during the "pushing" stage, they are solid. There are a few purposes behind this variety in firmness yet among the most squeezing is the exploitation of the elastic energy put away inside the muscles and ligaments. This empowers compliant actuators to accomplish execution which is beyond the realm of imagination with a traditional stiff robotic framework. [10] Another promising idea express the possibility of passive dynamic walking; even totally unactuated and uncontrolled systems can play out a steady step when walking down a shallow incline.

Anyhow, [11] researcher provided that additional actuation has many benefits such as power walking which can be possible through actuation at the feet and at the hips. Studies shows that passive and controllable gait cycles can be found for walking on zero slope, using impulsive pushing by the stance foot. Additional actuated degree around hip or ankle can also be necessary for the mechanism to turn. [40] Control of humanoid robots with flexible joints is generally more difficult than that of “stiff” humanoid robots, because the torques due to the joint compliance and dynamics linked to that are considered in dynamic analysis of robot. There are two strategies in control of robots with

flexible joints: one is to achieve accurate and robust link positioning under uncertainties and disturbances. [41] The other is to achieve accurate joint positioning. To develop inherently safe humanoid robots that share common workspaces with humans, physical compliance should be considered. Obtaining accurate link positioning results in stiff behaviors and may be dangerous when the robot physically interacts with humans. [45] Compliance surely have its advantages but additionally a few disadvantages, for example instigating commonly underdamped dynamics which crumble the stability margin and the precision of the robot yet additionally restricting the bandwidth, which was originally defined in closed loop system.

[46-47] These issues are defeated in mammalians, which show joint compliance because of the physical properties of muscles and ligaments, by using the characteristics of joint physical damping. Actually, the properties of passive compliance and damping present in the biological joints clarify why for example people can safely collaborate and be robust during impact (because of compliance) while in the meantime having the capability of accomplishing quick, smooth yet exact movement (thanks to physical damping). Robotics consists of many technical and scientific disciplines such as mechanical design, modeling, applied mathematics, automatic control, real time feedback systems, biomechanics etc.

This chapter would emphasis on some of the fundamental theory in the field of Robotics related to this work and would also present the principal concepts of modelling. It will help the reader to have a better idea of the terminologies used throughout the thesis.

## 2.2 Introduction

Throughout this work, Rollo, or simply Robot, refers to a Mechanical structure with flexible links in the legs performing biped locomotion. In general Robot is a computer controlled mechanical structure, programmed to perform some repetitive task in industries and in homes. Robots have different mechanical structures and configurations depending upon their tasks. The following presentation would be restricted to the robots performing a bipedal locomotion. A robotic mechanical structure is composed of bodies, known as links, connected with joints. The joints allow relative motion between two connected bodies. The most common joints are prismatic and revolute joints which provides linear and rotatory motion between the bodies. Robots which performs biped locomotion are usually consisted of the base (foot), which can be rigid block that mimics a natural human foot, which can be with or without wheels. With that connects the legs, trunk and then upper body.

Joints between the links determine the total degree-of-freedom (DOF) of the Robotic structure. According to Siciliano and Khatib [64] The space in which a robot can operate is called its reachable workspace and where it orients itself arbitrary is known as its dexterous space. Electrical motors actuate the joints by providing them with a necessary torque for the desired operation and allowing them to move. The position of the motor is fed back to the controllers which then find and fix the error relative to the reference position and output the torque accordingly.

## 2.3 Coordinate System and Transformation

In Robotics technological applications, a wide range of coordinate systems can be utilized to characterize where robot, its sensors, and different items belonging to the space are found. By and large, the area of an article in 3-D space can be

determined by position and orientation values. There are multiple possible representations for these values, some of which are specific to certain applications. Translation and rotation are alternative terms for position and orientation and govern by reference frames. Each frame consists of three orthogonal unit vectors $(xi, yi, zi)^T$ where one is in the direction of the joint rotation. To describe a reference frames rotation relative to another three angles, $(\phi 1_I, \phi 2_I, \phi 3_I)^T$, are used. A common setup known as synchronization. In this setup all the reference frame of fixed bodies is parallel to the world plane.

The rotational matrix describes the rotation between two coordinates frames. Rotation along *z-axis* is given by

$$R_z = \begin{bmatrix} cos\varphi & -sin\varphi & 0 \\ sin\varphi & cos\varphi & 0 \\ 0 & 0 & 1 \end{bmatrix}$$

The displacement between the two frames is described by a vector given below

$$d_b^a = (x, y, z)^T$$

Whereas general transformation matrix represents displacement and rotation between the frames in a same matrix. The matrix is *4x4* known as homogeneous transformation matrix.

$$T_b^a = \begin{bmatrix} R_b^a & d_b^a \\ 0 & 1 \end{bmatrix}$$

**2.4 Robotic Models**

This part will describe the kinematic and dynamic models in the robotics model, which are base to this work, the describe the relation between all the elements of the robot.

### 2.4.1 Kinematic Models

The kinematic models describe the motion without regard to the forces that cause it, i.e., all the time-based factors and geometrical properties of the motion. The position, velocity, acceleration, and higher order derivatives are all described by the kinematics as mentioned by Siciliano et al [64].

### 2.4.2 Robot Jacobian

Jacobian of robot is obtained by performing a derivation of the kinematics equation with respect to time. It provides the link between the joint and the linear and angular velocities of the end effector. It also provides the relationship between the joint torques and the resultant forces and joint applied by the robot body. Jacobian also used to check the singularities in solution.

### 2.4.3 Dynamic Models

The conditions of motion are imperative to consider in the structure of robots, just as in simulation and animation, and in the planning of control algorithm [65]. The models are figured in the joint spaces. The humanoid robot body comprises of successive connections. The principal connection indicates the reference frame. To disentangle the equations, the robot is considered as a biped model. It is practical to sum up these relations all through the entire robot body to consider the impact of upper body. The frames are settled by beginning from one of the robot feet as the reference base and after that proceeding to its shank, thigh and hip connections, and thereafter moving contrarily in the other leg to achieve its foot.

In Mu and Wu, 2004 [66] a Lagrangian approach was taken and it was found that the system dynamics could be described by Equation

$$\tau = A(\theta)\ddot{\theta} + B\left(\theta, \dot{\theta}\right)\dot{\theta} + C(\theta)$$

Where *A* is a matrix describing the system inertia, *B* is related to the centrifugal and Coriolis terms, *C* is a vector related to the gravity and $\tau$ is the external forces applied to the system. This equation is an inverse dynamical model describing the torques needed to make the biped robot undergo a certain motion.

$$\ddot{\theta} = A(\theta)^{-1}(\tau - B\left(\theta, \dot{\theta}\right)\dot{\theta} + C(\theta))$$

Equation above describes the acceleration of the biped robot under the effect of external torque. Input/output relation of the dynamical system can be seen from the given figure

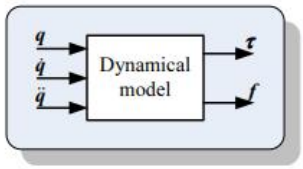


*Figure 1- Input/output relation of the dynamical system*

A real system has its flexibilities distributed over its entire body. So the dynamics of the model can range between being rigid and being elastic. In our context we would considered both so the overview of bot type of modelling is necessary.

#### 2.4.3.1 Rigid Dynamic model

There are several methods for obtaining a rigid dynamic model. The two most common approaches are the Lagrange formulation (Spong et al., 2006) and the Newton-Euler formulation (Craig, 1989). In a rigid dynamic model, the links and bodies are assumed to be rigid. The mass and inertia of the actuators and

gearboxes are added to the corresponding link parameters. The model consists of a serial kinematic chain of N links modeled as rigid bodies as illustrated in Figure 2 below.

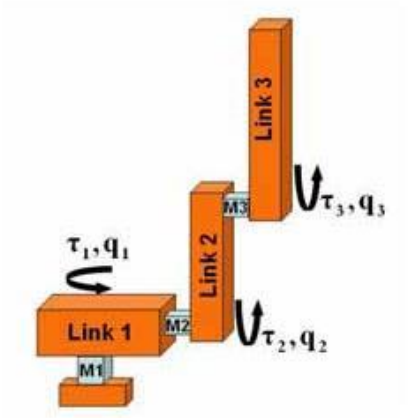


*Figure 2 – represents serial kinematic chain of N links modeled as rigid bodies*

The model can be solved by the equation given above in the general context.

### 2.4.3.2 Flexible Dynamic model

Bascetta et al [67] describes thee different levels of elastic modelling, one of which is Lumped Parameters Models. In which the elasticity is modeled by discrete, localized springs. With this approach, a link can be divided into a number of rigid bodies connected by non-actuated joints. Robot given in sec 2.3.3.1 can be modeled considering the presence of the springs in the middle of rigid bodies as shown in the figure below.

The flexible joint models can be driven by using a Lagrange equation same as the rigid model but with addition of stiffness and damping factors.

$$\tau = K(\theta_m - \theta) + D\left(\dot{\theta}_m - \dot{\theta}_a\right)$$

Where *K* and *D* are the stiffness and Damping matrix of order N. The potential energy of the springs must then be added to the potential energy expressions as

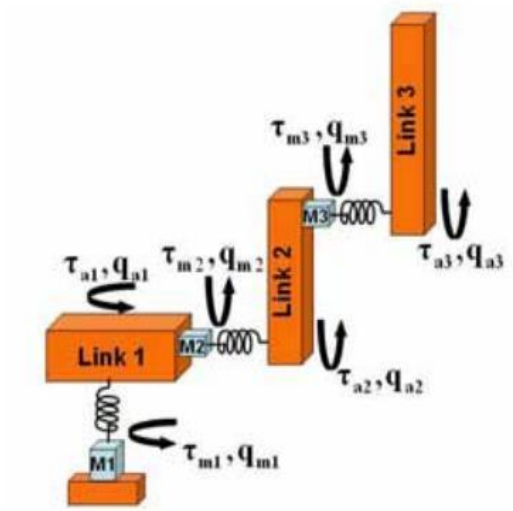


*Figure 3 - represents serial kinematic chain of N links modeled as rigid bodies with addition of springs*

$$\tau = K(\theta_m - \theta) + D\left(\dot{\theta}_m - \dot{\theta}_a\right)$$

Where *K* and *D* are the stiffness and Damping matrix of order N. The potential energy of the springs must then be added to the potential energy expressions as

$$V_s(\theta, \theta_m) = \frac{1}{2}(\theta - \theta_m)^T K(\theta - \theta_m)$$

for rotating actuator, the compensation of kinetic energy should be added as well.

#### 2.4.3.3 Inverse and Forward Dynamics.

As indicated by E. Otten [68] equation of motion gives the relation between motion and forces which led us to either the problem of reconstructing the internal forces/torques from the motion and known external forces, which is called the ‘inverse dynamics problem’, or on the other hand computing movement from known inward forces/torques and resulting response forces, which is known as ‘forward dynamics problem’.

To predict the resulting movements, Forward Dynamics utilizes torques/forces of the joint. Inverse dynamics is based on the subject's motion and a body model in order to calculate the forces needed to generate this movement. Inverse Dynamics is used as a form of biomechanical modeling much more frequently than Forward Dynamics. Besides computing forces to achieve a required kinematic motion, Inverse Dynamics also helps to calculate the forces when external forces are engaged. External ground forces must be taken into account when an articulated body walks on the ground. Even leaning on a wall results in normal forces. Inverse dynamics can take in account for all this external forces.

## 2.5 ROLLO in detail

ROLLO was implemented as part of the Brainhuro initiative which sought to realize, using Brain Computer Interface (BCI) techniques, a humanoid robot connected using brain computer interface (BCI) technologies [48] and can be managed by individuals suffering from amyotrophic lateral sclerosis (ALS) illness, with very limited or no mobility.

In the initial phase of the project, the robot was conceived with the same characteristics of the SABIAN robot [49-52]. However, the large size and

complications of the SABIAN robot in the true setting could, nevertheless, restrict the practical use of the robot. The lack of security for individuals around a SABIAN-like machine was another disadvantage. A small and simple robot called ROLLO with the same movement functionality of SABIAN has been designed to solve these limitations and consider the objective of the Brainhuro project (that is, a robot capable of implementing alternative biped movement on a flat surface and of transmitting pictures to patients). The ROLLO robot presently in patent pending condition may be manipulated by human neurons using commercially accessible BCI technologies, but also by other natural device devices (e.g. smartphones, phones, pcs and joysticks).

### 2.5.1 Structure and Design

The robot with the height around 1000 mm, weight around 10 kg can move using only two gear motors (see Fig. 4), the figure shows the ROLLO robot used as a biped robot controlled by external devices (e.g. joystick) (see Fig. 1(a)), and by a BCI system (Fig. 1(b)), one for each leg, and each leg is constituted by a flexible structure. The two legs are identical and each one is constituted by two (see Fig. 1(a)) or more springs (see Fig. 1(b)), one gear motor, one battery, two side wheels (external and internal) colligated to the shaft of the gear motor and two free wheels (frontal and rear) used to avoid falls. Springs or rigid component modules can be added to each leg in order to have different combinations of motion. A human-like motion of the robot can be achieved using one spring in proximity of each human-like joint (ankle, knee, and hip) and rigid elements in proximity of each human-like link (thigh and shin).

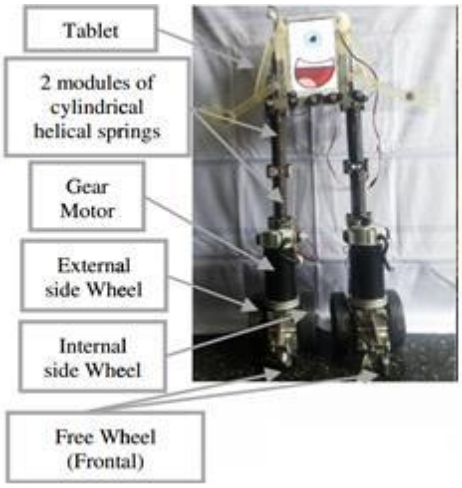


*Figure 4- ROLLO [54]: first prototype used as a biped robot controlled by BCI systems.*

. ROLLO can be moved in a rectilinear or curvilinear way. The rotation can be obtained either by fixing the external wheel to the shaft and using a bearing between the central hole of the internal wheel and the shaft of the gear motor or fixing each wheel (external and internal) to the shaft of the gear motor and having two driving wheels in each leg; in this case, the bipedal rectilinear motion and the rotation are both possible only thanks to the flexible structure of the robot. In each leg, other two free wheels are present respectively in the frontal and rear part of the leg (see free wheel in Fig. 1(a)); they are not fixed and can be moved around the axis perpendicular to the surface where the robot is moving, and they are used only to avoid falls.

A battery is used in each leg as power supply allowing the motion of the robot for two hours at the maximum speed. In each leg a driver, with a switch, controls the connection between power supply, motors, and the electronics positioned behind the tablet. The webcam of the tablet is the camera used for the transmission of the images between the robot and the patient/user. The tablet, the electronic hardware, the arms, and the hands of the robot are fixed to the

structure attached to the springs. The robot can rotate moving the wheels of each foot in the opposite direction. The altitude of the robot can also be modified by varying the number of the elastic modules in each leg. Figure 1(b) shows ROLLO with three elastic modules (cylindrical helical springs) in each leg and a tablet used to reproduce the head. Arms and hands are not yet active.

Figure 2 shows some pictures of the ROLLO robot developed by the [54] Humanot Company during the open ceremony of Ericsson Innovation Day 2015. ROLLO has been used as a presenter during the opening ceremony and has been controlled using a BCI system composed by a sensorized coif, available in commerce and developed by the [55] Liquid Web Company.

Figure 3 (on the left) shows a patient affected by amyotrophic lateral sclerosis (ALS) disease in his house while controlling the direction of movement of ROLLO robot using a BCI system. The patient may explore his house on Tablet 2 connected to the webcam of Tablet 1 mounted on the robot directly controlled by the patient. In the first step (see Fig. 5 on the right), the communication between the patient's brain, the BCI system and the ROLLO robot has been calibrated by a human assistant. In the second step (see Fig. 3 on the left), the human assistant mounted the sensorized coil on the head of the patient.

The basis for the novel concept implemented in ROLLO relies on previous works performed by the authors on dynamic balance of advanced biped robots and presented in Refs. [56] and [57]. In ROLLO, the main elements of the mechanical structure of the legs are springs, connected in series in a way that allows the robot to perform an alternate biped walking pattern and to remain in a standing position also when the motors are not active. With this approach, the motion is made possible thanks to only two motors, positioned within the

leg structure and directly connected with the wheel rotation. In order to move the robot in a rectilinear direction and with a constant speed, the two gear motors must rotate with the same direction. In this case, two kinds of motions are possible: one with the legs moving together, and one with an alternate motion of the legs, in a way that resembles the human walking pattern. The coordination of the motor motion is managed by the on-board electronics. On the contrary, if the speed value of the gear motors is the same and the direction of rotation of each motor is opposite, the robot will rotate around an axis perpendicular to the plane of motion, thanks to the overall structure that keeps the legs together. ROLLO architecture resemble to the one of the T.P.T. robot [58] architecture in the terms of electronic design, a simple robot conceived as a taekwondo personal trainer robot [59] and developed by the Humanot Company [54].

### 2.5.2 Springs in ROLLO

The lower part of the robot is constituted by two flexible legs, composed by cylindrical helical springs used in an unconventional way. More in detail, cylindrical helical springs are usually used for compression/extension behavior in the same direction of the axis of the spring (see Fig. 4). In the presented robot, the cylindrical helical springs, integrated in the structure of the legs, are used to develop a passive motion exploiting a torsional and flexural behavior of the springs. While the conventional compression/extension behavior of cylindrical helical springs is a well-known problem in the scientific literature, a torsional and flexural conduct incorporates a progressively mind-boggling computation. Della Pietra [60] in 1976, dissected, both hypothetically and tentatively, the coupling among torsional and flexural strains in cylindrical helical springs exposed to excitation along their very own axes. The systematic examination, created based on the hypothesis till 1976, had demonstrated the presence of two arrangement of resonance conditions: the first compares to the one definitely

known for the pivotal vibrations, the other one was with respect to the vibrations comprised by the turns of the coil around the spring axis. The trial look, completed by [60], around two springs having various attributes and which are exposed to diverse preloading of the assembly, has demonstrated that the coupling among torsional and flexural strains is substantially more complex than the one shown by theory, because of the presence of lateral deformations of the spring. More recent papers [61,62] propose a free vibration analysis of cylindrical helical springs with non-circular cross-sections and investigate helical springs subjected to axial loads under different dynamic conditions.

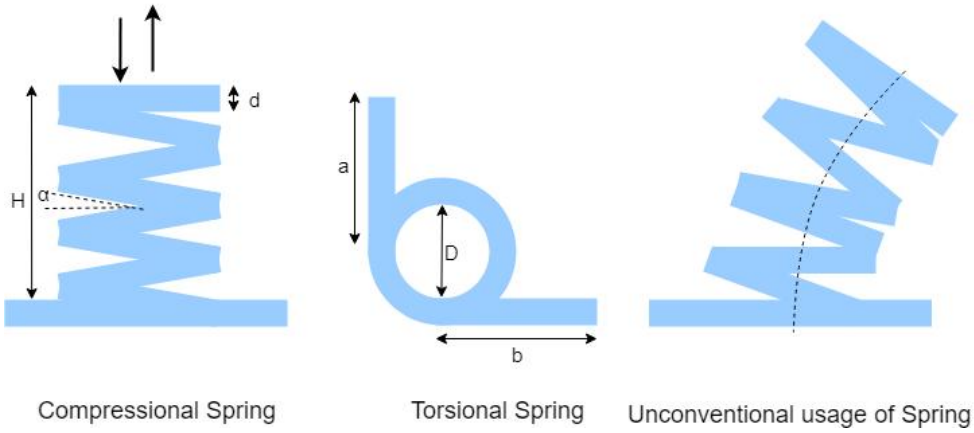


*Figure 5 – represents the torsional and compressional parameters and the use of springs in an unconventional way*

A typical helical spring, as shown in Fig. 4, is a spiral wire or rod with mean diameter of coil $D=2R$, wire diameter $d$, number of active coils $i$, helical degree α, uniform pitch of the helix $p=\pi*D*tan\alpha$, free length $H=i*p$, length of the wire or rod $L=\pi*D*i$. If an axial force is applied on the spring, a combination of torsional and flexural strains is generated on the wire of the spring. Many details about the nonlinear behavior of the spring in this or other conditions can be found in Refs. 60–63. In order to simplify the discussion and to obtain a preliminary estimation of the stiffness of the ROLLO's legs, we show in

following some conventional assumptions used to define the stiffness of the spring (K) (valid also if the spring is used in an unconventional way).

In particular, we used a cylindrical helical spring excited with a load perpendicular to the axial direction. The first conventional assumption is that if a helical degree α is small (<8°) trigonometric functions can be simplified (*cosα=1, sinα=0*) with a 1% error. The second conventional assumption used in many experimental applications is to assume the flexural and torsional behavior of the cylindrical helical spring like the behavior of a torsional spring.

A simple method to calculate the behavior of the cylindrical helical spring is to consider only the torsional load *Mt* on the spring. The maximum strain on the wire is $\tau_{max}$ where *Jp* is the inertial moment:

$$\boldsymbol{\tau_{max} = \frac{M_t}{J_p} \cdot \frac{d}{2}} \quad \textbf{(1)}$$

In order to calculate the stiffness of the spring, the work generated by the force is compared to the elastic work accumulated on the wire. *F* is the torsional force which produces a *f* displacement; φ is the rotation induced by $M_t$; *G* is the tangential module.

$$M_t = F \cdot R, \quad (2)$$

$$\frac{1}{2} \cdot F \cdot f = \frac{1}{2} \cdot M_t \cdot \phi = \frac{1}{2} \cdot M_t \cdot \frac{M_t \cdot L}{G \cdot J_p} = \frac{1}{2} \cdot F \cdot R \cdot \frac{F \cdot R \cdot 2 \cdot \pi \cdot R \cdot i}{G \cdot \frac{\pi \cdot d^4}{32}}, \quad (3)$$

$$K = \frac{F}{f} = \frac{G \cdot d^4}{64 \cdot R^3 \cdot i}. \quad (4)$$

With the same assumptions, and referring to Fig. 4 where a flexural moment $M_f$ is imposed on the spring, the flexural degree ϕ of the spring can be calculated, including Young module E and inertial moment *J*:

$$M_f = P_1 \cdot a = P_2 \cdot b, \tag{5}$$

$$\varphi = \frac{M_f \cdot i \cdot D \cdot \pi}{E \cdot J}. \tag{6}$$

If $J = J_p$, the parameters to find the springs for the legs of ROLLO are shown in the following and are functions of *i, D* and *d*:

$$f(i, D, d) = \frac{i \cdot D}{d^4} = \frac{E \cdot \varphi}{64 \cdot M_f}. \tag{7}$$

Moreover, while most of the biped robots available in commerce and literature need power supply in order to keep a standing position, ROLLO, by means of the cylindrical helical springs integrated in the structure, can keep an upright position without the activation of the power supply. This feature allows one to reduce the amount of energy spent by the robot during motion. Another characteristic of the robot is to combine the flexibility of the structure with the biped wheeled system allowing many combinations of steps. For example, the robot can move with an alternated step of each foot with respect to the other one, or with a common motion of the two legs, with the whole robot moving as a traditional wheeled robot. All these motions can be performed at eight different velocities.

*Chapter 3*

# Implementation and Control of the Robot

Designing and control a robot manipulator and to achieve a highest possible efficiency is one of primary focus of the Robotic industry and researchers attached to this field. In this experimental study, ROLLO robot [54] is dynamically modeled and Control architecture for the position control has been defined. The main aim of this study, is to perform a controlled biped locomotion using a flexible links between the ankle, hip and knee joints.

## 3.1 Implementation

This part briefly presents the implementation of the ROLLO robot in simulation environment according to the description provided in chapter 3. All the designing and simulation were performed on same machine, with the following specifications: -

- Operating System: Windows 10 Pro 64-bit
- System Manufacturer: Acer
- System Model: Acer Aspire E15
- BIOS: InsydeH2O Version 03.72.38F.65
- Processor: Intel(R) Core(TM) i7-6500U CPU @ 2.5 GHz (4 CPUs), 3.1GHz
- Memory: 12288MB RAM

### 3.1.1 CAD model using Solid Works

Solid Works 2017 has been utilized to create a 3d virtual model of the ROLLO [54] robot by the specification almost similar to the one used for the real test. The model is equipped with the flexible legs using the compression springs and

the foots are designed using the Rod which is connected to 4 wheels, 2 side wheels are the main wheels which would be actuated by the motors. Whereas the 2 free wheels attached with pin in the front and the back to provide the extra stability to the robot and help in standing without the actuation, which will eventually help us to save the energy when the actuation is not needed. The 3d model of the Rollo robot is presented in figure (5) in the solid work environment.

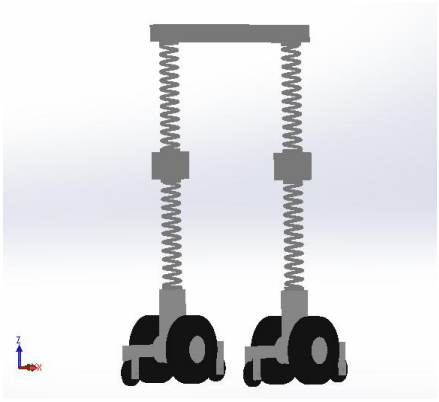

*Figure 6- shows the side view of 3d model of the ROLLO Robot in the Solid works CAD assembly and environment. The robot is in configuration 1: two springs in each leg.*

The mating of the different components and subassemblies were added in the solid works. The different mates between the components are placed to fulfill the requirements of the kinematic chain to provide constrained or desired motion. Eventually, the final model of ROLLO was exported using the Simscape multibody add-in for the Solid works, which export the model in its ".xml" file.

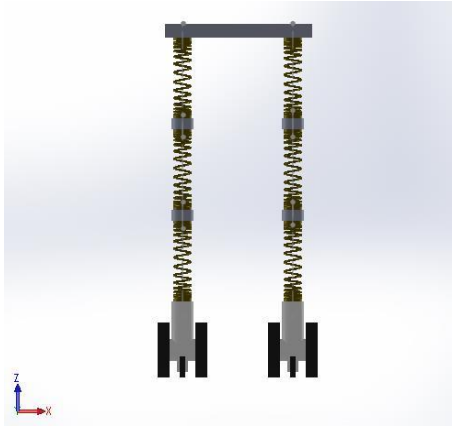

*Figure 7 - shows the 3D model of the ROLLO [54] Robot CAD assembly in the Solid Works environment. The robot is in configuration 2: three springs in each leg*

### 3.1.2 Defining Robot in Simscape MATLAB

The ".xml" file contains the position, orientation, density inertia and many other details of the components and assemblies of Rollo model was imported in Simscape multibody environment using 'smimport' function. This function automatically transfers all the specification of the ROLLO defined in the 3D software to Simscape multibody simulator.

The higher level hierarchy Simscape multibody environment of the robot is shown in the figure (7). There is the 'ROLLO' block which consists the different body blocks of the robot whereas the 'World Plane' has the definition of the world parameters. These blocks are connected with 6-DOF which allows the robot with 6 degree of freedom to move in the world environment. 6-DOF joint also allows us to define the damping coefficient between ROLLO and world. The damping coefficient along the translational axes is equal to $0.25\ N/(m/s)$ whereas for the rotation it is equal to $0.25\ N*m/(rad/s)$.

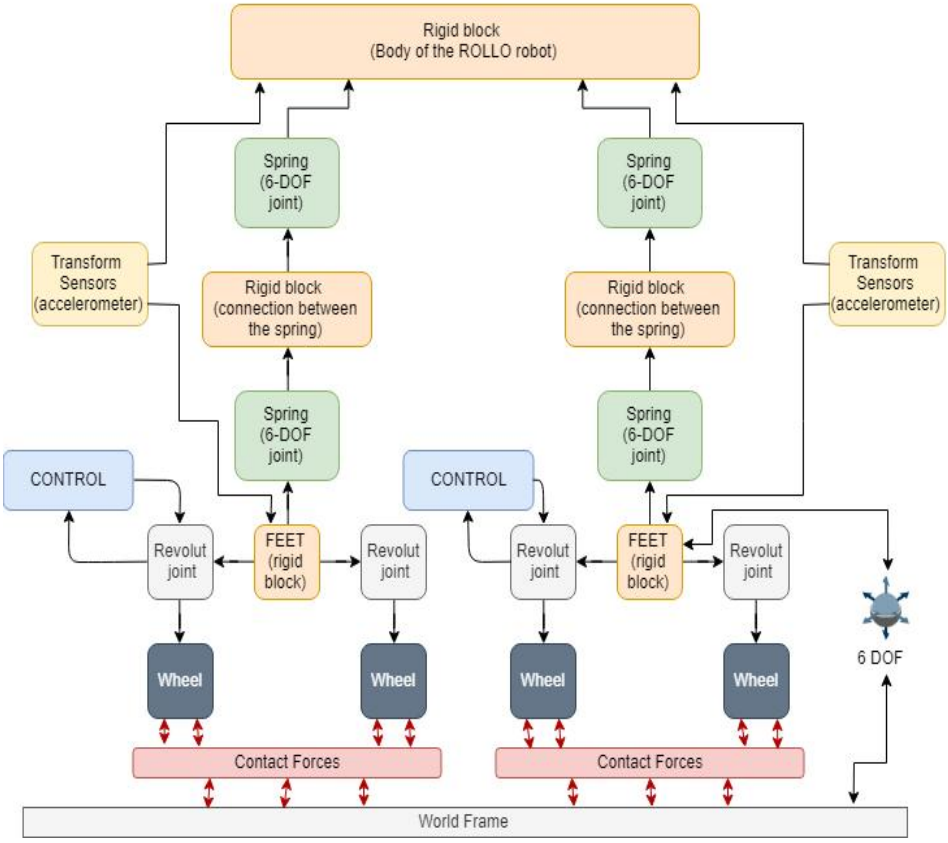


*Figure 8 - shows the 'ROLLO' [54] block diagram in the Simscape multibody environment present in a virtual World frame.*

### 3.1.2.1 World Frame

Inside the World Frame subsystem, you can find a World or ground frame, World frame is the ground of all frame networks in a mechanical model.

The mechanism configuration block sets mechanical and simulation parameters. Where we can specify the uniform gravity for the entire mechanism in the desired axis. We can also specify the perturbation values by setting up the linearizing delta. The solver configuration block defines the solver setting for the simulation.

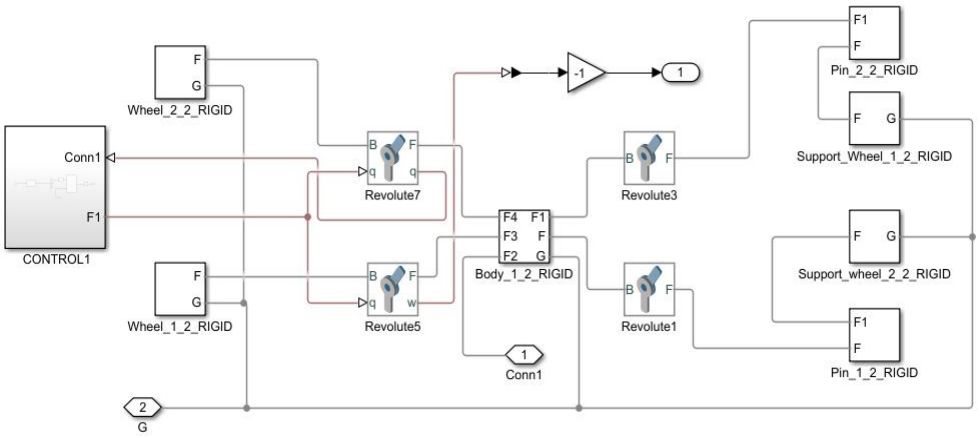


*Figure 9 - shows the Wheel subsystem present inside the ROLLO subsystem*

The main block present inside foot figure (9) is the body with which all the components are attached. Wheel and support wheel are attached to the body by the mean of the revolute joint. Which has one rotational degree of freedom represented by revolute primitive. The two main right and left wheels have position actuation provided to revolute joint block. To receive a human like gait we pass the motion input in the revolute joint and let it compute the torque automatically. The revolute joint also sense the position while present in simulation and feed it back to the controller.

### 3.1.2.2 Contact Forces

The contact forces added to the wheels of robot are the one which constraint the robot body against the world plane. These contact forces are provided by the Contact_force_library from math works. They are discreetly added to every wheel of the Robot. They use the dimension of wheel and the plane to induce the forces between them. The following diagrams and text present the Simscape Multibody Contact Forces Library's configuration on force laws. It applies to contact forces in 2D and 3D.

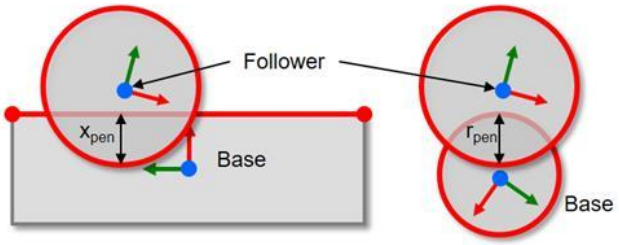


*Figure 10 - Contact forces between Circle to plane and circle to circle.*

**Linear**

A linear spring-damper resists penetration. Damping force is 0 as penetration decreases. Force is applied only along the direction of penetration.

Circle to Line

$$F_x = \begin{cases} k*x_{pen}+b*v_{pen} & x_{pen}>0,\ v_{pen}>0 \\ k*x_{pen} & x_{pen}>0,\ v_{pen}<0 \\ 0 & x_{pen}<=0 \end{cases}$$

$$F_y = 0$$

Circle to Circle, Ring

$$F_r = \begin{cases} k*x_{pen}+b*v_{pen} & r_{pen}>0,\ v_{pen}>0 \\ k*x_{pen} & r_{pen}>0,\ v_{pen}<0 \\ F_r = 0 & x_{pen}<=0 \end{cases}$$

Where k is the contact stiffness (Spring stiffness for force law) and b is the contact damping (damping constant for force law).

**Nonlinear**

Same as linear except:

1. Stiffness force increases exponentially with penetration $k*(X_{pen})^e$, where e is parameter *Penetration Exponent*.
2. Damping force increases gradually during initial penetration $b*v_{pen}$*(Smooth Step), where Smooth Step is a polynomial whose value increases from 0 to 1 as the penetration increases from 0 to parameter Penetration for Full Damping.

The parameters which have been used in the Sphere to plane contact force block to define the contact realistically are given in the following table.

| Parameters | Value |
|---|---|
| Force Law | Linear |
| Contact Stiffness (N/m) | 5000 |
| Contact Damping (N/(m/s)) | 500 |
| Friction Law | Stick slip Continuous |
| Kinetic friction coefficient | 0.5 |
| Static friction coefficient | 0.7 |
| Velocity threshold (m/s) | 0.001 |

*Table 1 - Contact forces parameters.*

In addition, contact force block also takes the data of the wheel radius and dimension of the world plane to apply the forces accordingly.

#### 3.1.2.3 Springs

Flexible links between the leg joints are realized using a 6 degree of freedom joints. This joint has three translational and three rotational degrees of freedom represented by three prismatic primitives' axes along a set of mutually orthogonal axes, plus a spherical primitive. This joint allows unconstrained 3-D translation and rotation. The follower origin first translates relative to the base frame. The follower frame then rotates freely, with the follower origin as the pivot.

Ports B and F are frame ports that represent the base and follower frames, respectively. The joint direction is defined by motion of the follower frame relative to the base frame.

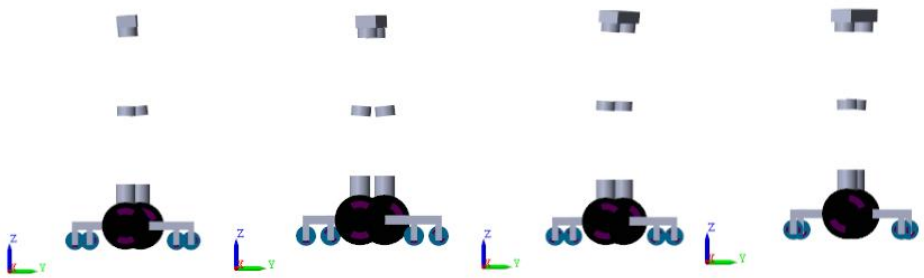

*Figure 11 - Demonstration of the flexible links performing the forward gait in the configuration with 2 springs in each leg*

Exploiting the properties for the internal mechanics of this joint a spring behavior is achieved. This joint is not visible physically but provides the relevant force and torques to the follower frame with respect to the base frame. Specifications of the joint to achieve a spring behavior are given in the following table.

| Parameters | Value |
|---|---|
| Spring stiffness in x (N/m) | 10400 |
| Spring stiffness in y (N/m) | 10400 |
| Spring stiffness in z (N/m) | 10400 |
| Spring stiffness in spherical primitive (N*m/deg) | 0.18 |
| Spring equilibrium position in z(m) | 0.29 |

*Table 2 - Springs Parameters.*

### 3.1.2.4 Mechanics Explorer

Mechanics Explorer is a tool provided by the MATLAB in a Simscape Multibody environment. It lets you explore and visualize the multibody in the

virtual world environment which have been defined in the Simulink and MATLAB.

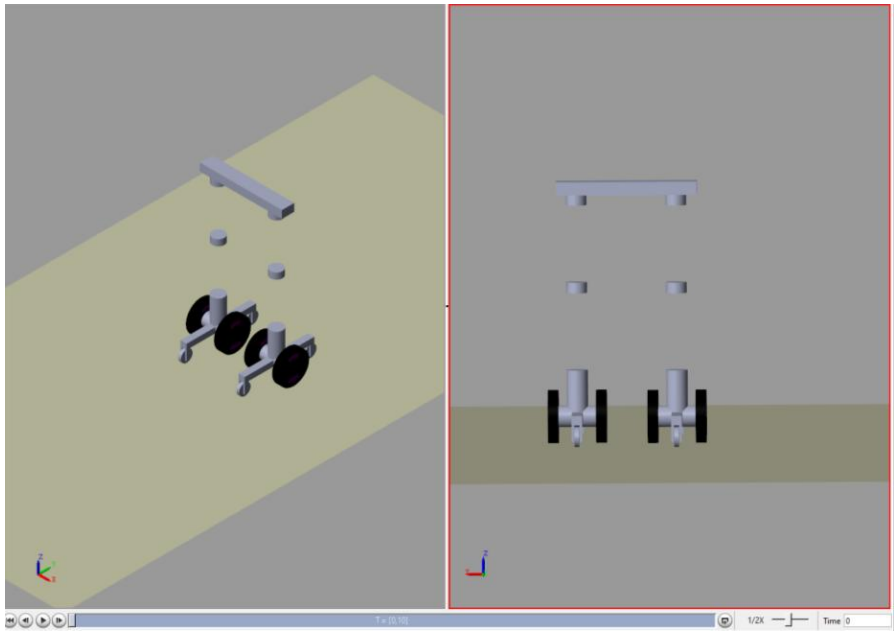

*Figure 12 - shows the updated diagram of the robot viewed in built in 3D explorer of the Matlab called mechanics explorer. The robot is in configuration 2: three springs in each leg.*

### 3.2 Control Architecture

The issue of balanced walking is the most basic issue for humanoid biped robots, and present solutions are still need to be reconsidered for numerous world applications.

The humanoid control approach is essentially distinct: One approach assumes very precise models of the actual robot and its environment. The humanoid control approach is essentially distinct: One approach assumes very precise models of the actual robot and its environment. A straightforward and abstract

model of dynamic behavior is another starting point to reach concordance with reality with feedback control. The third direction of studies can be subsumed as control methods inspired by nature. These include techniques based on neural networks, fuzzy logic or genetic algorithms and are often motivated by the concept of robots acting and reacting to unforeseen occurrences in unknown settings.

### 3.2.1 Low-level Joint Control

The precision of low-level joint controller's trajectories is a very important component of humanoid robot control. The low level joint controller algorithm is utilized. The main functionality of this Low level joint is to minimize the oscillations around ankle and hip joint by preventing the hard stop in each gait and by Smoothing the input trajectory by exploiting the linear to curve fitting techniques. The problem is given by the evaluation input positions (Gait) provided as a motion input for each joint. By giving the angular position in the time we calculated the angular velocity and eventually the linear velocity of the robot. The different velocities configurations are given in the following table.

| Parameters | Value |
|---|---|
| **Velocity 1 (m/s) Lowest** | 0.025 |
| **Velocity 2 (m/s)** | 0.05 |
| **Velocity 3 (m/s)** | 0.1 |
| **Velocity 4 (m/s) Highest** | 0.2 |

*Table 3 – different velocities configurations which were used for the ROLLO simulation*

By the given positions and the desired time durations the blend times, straight segment time, Slopes (velocities) and signed accelerations are computed using the

linear interpolations as given in the following source.

https://see.stanford.edu/materials/aiircs223a/handout6_Trajectory.pdf

The summary of the solutions evaluated in joint space and Cartesian space is mentioned below.

- Trajectories in terms of position and velocities are fed to the control system.
- Path generator computes according to the path update rate.
- In joint Space
    - Changes the set of coefficient at the end of each segment by using the cubic splines.
    - check on each update if you are in linear or blend portion and use the formula appropriately.
- In Cartesian Space:
    - Calculate Cartesian position and orientation at each update point using same formulas
    - Convert into joint space using inverse Jacobian and derivatives

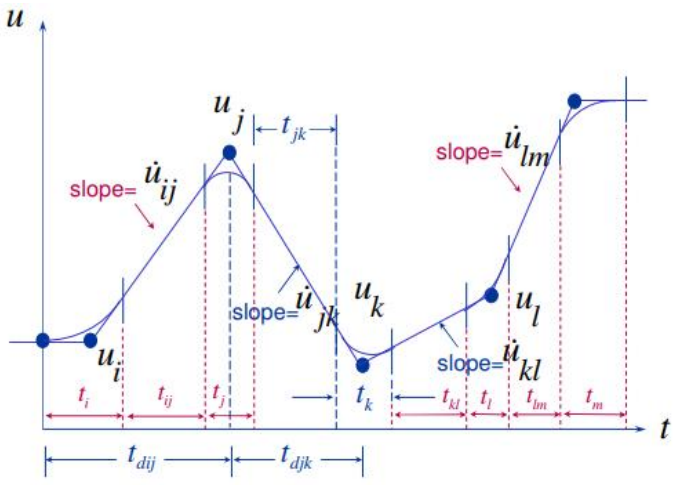


Figure 13 - *Represents a linear interpolation with blends for the several segments*

This low level control is developed in Matlab using Matlab function blocks that run our trajectory evaluation and both of them passed in the simulation

time using the clock. The right leg uses the time as is and the left leg uses the delay of the half of the gait period.

In the figures below presents the comparison between the joint angles in degrees. The figure (1) is just a linear and linearly interpolated waypoints whereas the figure (2) depicts the smoothed out cubic spline trajectory.

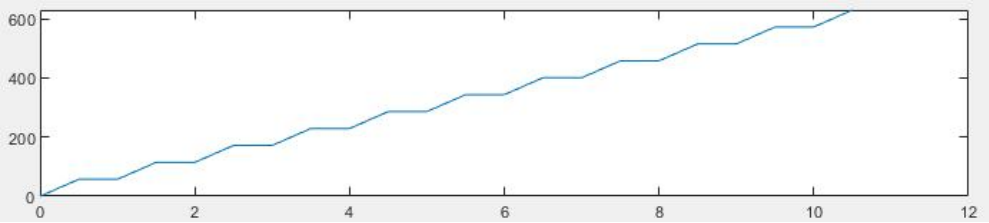


*Figure 14 (a) - represents the motion profile (angle of joint w.r.t time) of right leg defined for the Velocity 4 = 0.2m/s before the Low-level joint control*

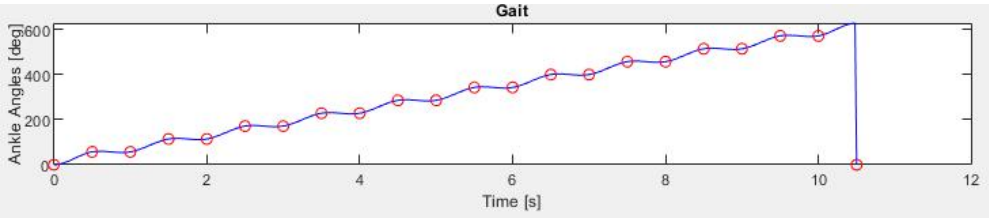


*Figure 15 - represents the motion profile (angle of joint w.r.t time) of right leg defined for the Velocity 4 = 0.2m/s after the low level joint control*

The difference is not so quite evident but if we would look at the difference in torques the changes will be evident. The result is discussed in the chapter 4 *Figure 34* and *Figure 35*. By smoothing our curves, we make sure that our required torque doesn't change very quickly thus preventing the hard stop.

### 3.2.2 Dynamic Filters

Humanoids robots are required to make a variety of motions in dynamic environment, a promising approach was presented by Yamane and Nakamura [69] and have been used in a presented simulation of ROLLO robot conveniently by using along the Passive-Dynamic behavior of the springs.

The fundamental idea is to only define joint trajectories for certain joints and calculate Cartesian paths from the specified path for the single, arbitrarily chosen set points of the robot. The Cartesian movements are then returned to a joint movement. Since the optimization is local, it is not necessary to understand the total trajectory during the filtration process, therefore the trajectory may be altered during execution. Another benefit is that the approach can be used without restrictions in any movement.

The motion equations are provided as a reference input to the low pass dynamic filter which is then connected to the PID controller in a feedback manner to track the motion. The ankle joint acceleration can be completely different from the preference motion. To make sure that the result come closer to the reference result with the minimum oscillations we define the desired acceleration by following relation to the PID controller parameters.

$$\ddot{\theta}_G^d = \ddot{\theta}_G^{ref} + K_{DP}\left(\dot{\theta}_p^{ref} - \dot{\theta}_p\right) + K_{PP}(\theta_p^{ref} - \theta_p)$$

Where $K_D$ and $K_P$ are the coefficient matrices and the parameters of the PID controller. The controller block in Simulink are shown in the following block diagram.

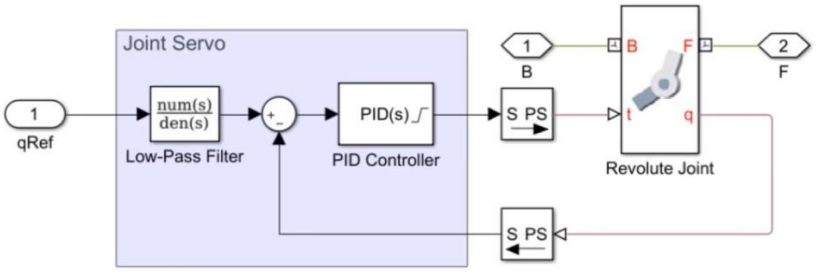


*Figure 16 - represents Controller block diagram in Simulink used for the simulation of ROLLO robot*

The tuning of the PID controller is done using a robot as a plant, and by considering different disturbances as shown in the figure 19. The controller is designed to follow an optimal behavior, while containing the overshoot, settling time of the robot in the suitable values. The following table details the controller parameters.

| Parameters | Value |
|---|---|
| $K_i$ | 4 |
| $K_p$ | 20 |
| $K_d$ | 8 |
| *Motion time constant* | 0.025 |

*Table 4 – Controller Parameters for PID*

These parameters are obtained by putting a controller in a closed loop with a plant and the following issues were considered while designing controller.

- steady state behavior of the tracking error e=r- y in the presence of the reference r
- steady state behavior of the output yin the presence of the disturbances.

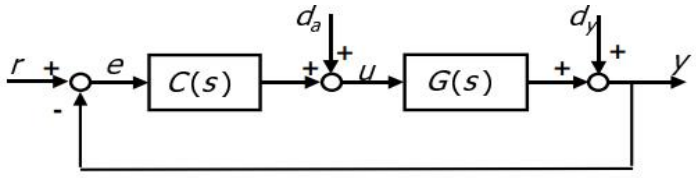


*Figure 17 - represents the general feedback system consist of plant and controller*

The difference in the wheel actuation before applying the controller and after controller is shown in the figure 20. The detailed results and the effects on the robotic stabilization and motion are discussed in chapter 4 *Figure 34* and *Figure 35*.

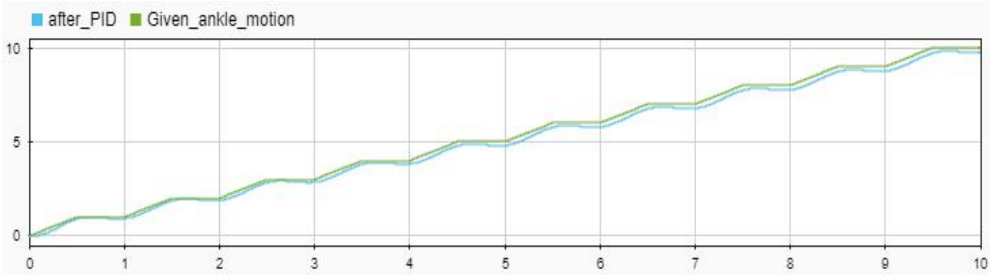


*Figure 18 - represents difference between the given ankle motion (green) versus output of the PID (blue)*

### 3.2.3 Passive-Dynamic Walkers

In ROLLO simulation low level motion input control and then dynamics filters have been used on the foots consisted of wheel, whereas the upper body is considered as dynamic passive walker.

Passive-Dynamic Walkers have no motors or controllers, yet they manage to follow the human like motion. The main factor behind is the natural dynamics of these elements. They have been mechanically designed that under the minimum actuation they can manage to settle themselves in the steady state and perform periodic gait.

*Chapter 4*

# Simulation and Results

The ROLLO robot simulation depended on the work given in [3]. An inventive structural approach centered at rearranging the control of biped humanoid robot's, in a way to accommodate him in a household situation. The approach depends on the execution of a passive flexible structure in establishing the robotic legs, which are then connected to the wheeled feet. The differently utilized cylindrical helical springs in the adaptable structure of the legs permits biped robot ready to accomplish a human like alternating leg motion having just two dynamic motors and staying in a standing position likewise when the motors are switched off.

## 4.1 Protocol of the simulation

Different experimentations have been performed on the ROLLO robot while considering the specific aims and focused on the specific result. The parameters of the ROLLO robot are tuned as the Domestic environment. Thus, the experimentation was focused on the analyzation of the oscillations and the angles of the robotic body. These results have been obtained while performing the forward motion with alternate steps of the legs and also during the rotation of $360^{o}$.

The measurements of oscillations and angles are performed by utilizing the transform sensor block. This block consists of a sensor that measures the spatial relationship between two frames, which in this case is between ankle and ground frames or hip and ground frames. It can measure different parameters, which

consists of rotational and translational position, velocity, and acceleration. The sensor can measure these parameters between any two frames in a model. Measurement frames include World frame as well as rotating and non-rotating base and follower frames.

The transform sensor block is attached at the right leg. One is placed at the end of the springs and start of the wheel body and the other is placed at the hip joint between the spring and upper body connection. The transform block is shown in the figure below.

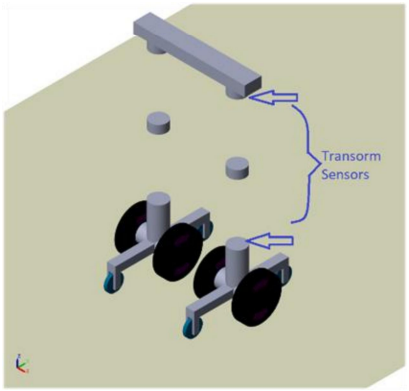


*Figure 19 - the position of the two accelerometers (1 and 2) on the ROLLO robot in Configuration 1 (two springs for each leg)*

### 4.2 Results

For better understanding of the results two different model configurations are realized.

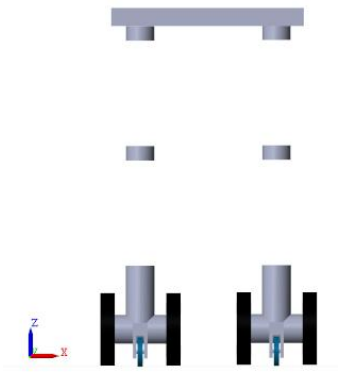

*Figure 20 - the configuration 1 (2 springs in each leg) of the ROLLO robot for the simulation in MATLAB*

Configuration 1 is composed of 2 springs in each leg whereas configuration 2 is composed of 3 springs in each leg. The both configurations are shown in the figure 22 and figure 25.

Some of the results related to the accelerations of the hip and the ankle joints for configuration 1 is shown in the figures below whereas the summary of all the acceleration results related to forward motion in configuration 1 is defined in the table.

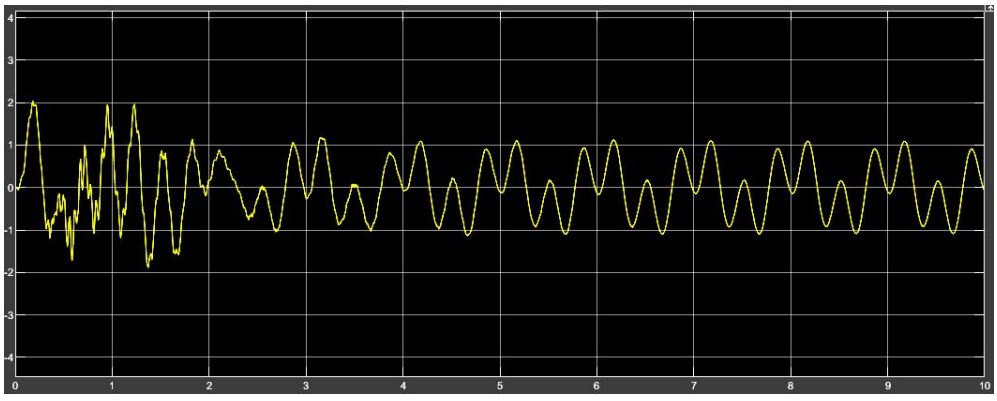


*Figure 21 - Hip acceleration in the forward direction (y-axis) in this case. The P2P value for the acceleration is calculated as 3.881 m/s$^2$ and STD is 0.7030. The velocity is 0.2m/s.*

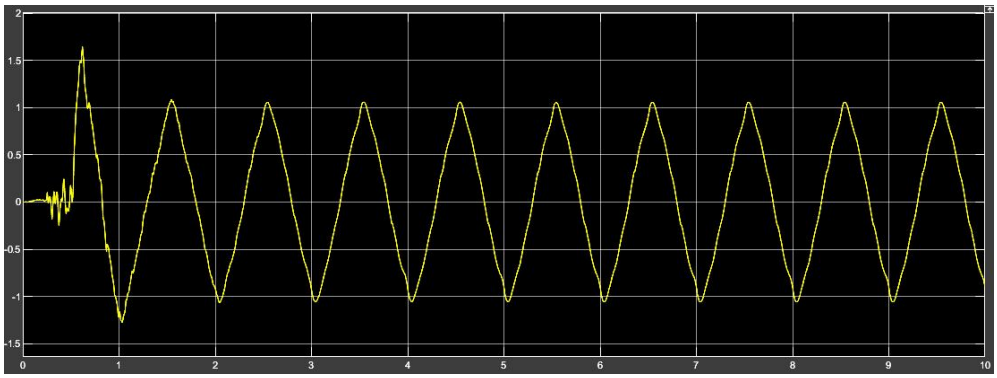


*Figure 22 - ankle acceleration in the forward direction (y-axis) in this case. The P2P value for the acceleration is calculated as 2.937 m/s. the velocity is 0.2m/s.*

The acceleration results related to the different configuration related to the different velocities are detailed in the tables below. Important thing to note here is that all the results are given in the ($m^2/s$), P2P defines the peak-to-peak value of the acceleration i.e. the difference between the highest and lowest values in acceleration and STD defines the standard deviation in the acceleration. In summary P2P value gives the information about the highest oscillation obtained during the motion while STD accounts for the mean oscillations calculated throughout the motion.

| **Axes** | | **$v_1$(0.025 m/s)** | | **$v_1$(0.05 m/s)** | | **$v_1$(0.1 m/s)** | | **$v_1$(0.025 m/s)** | |
|---|---|---|---|---|---|---|---|---|---|
| | | Foot | Hip | Foot | Hip | Foot | Hip | Foot | Hip |
| **X** | P2P | 0.433 | 1.268 | 1.110 | 1.762 | 1.384 | 1.915 | 1.438 | 2.248 |
| | STD | 0.015 | 0.069 | 0.0164 | 0.089 | 0.014 | 0.106 | 0.115 | 0.167 |
| **Y** | P2P | 0.505 | 0.617 | 0.856 | 1.173 | 1.528 | 2.137 | 2.901 | 3.881 |
| | STD | 0.084 | 0.092 | 0.167 | 0.182 | 0.334 | 0.365 | 0.667 | 0.703 |
| **Z** | P2P | 0.415 | 0.839 | 0.438 | 0.956 | 0.486 | 1.055 | 0.529 | 1.301 |
| | STD | 0.022 | 0.618 | 0.0249 | 0.693 | 0.024 | 0.732 | 0.1297 | 0.851 |

*Table 5 - Accelerations during a forward motion in Configuration 1.*

After this test the robot was assembled in a configuration 2, where one spring is added to each leg and it went through the same test as did in the configuration 1.The ROLLO robot in the configuration 2 is shown in the *Figure 23* below.

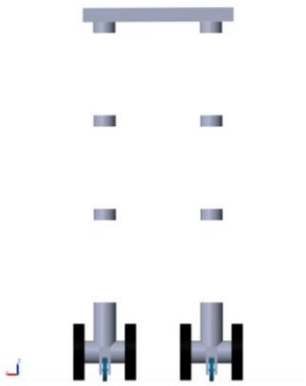

*Figure 23 - Configuration 2 (3 springs in each leg) of the ROLLO robot for the simulation in MATLAB*

Some of the results related to the accelerations of the hip and the ankle joints for configuration 2 is shown in the figures below whereas the summary of all the acceleration results related to forward motion in configuration 2 is defined in the table.

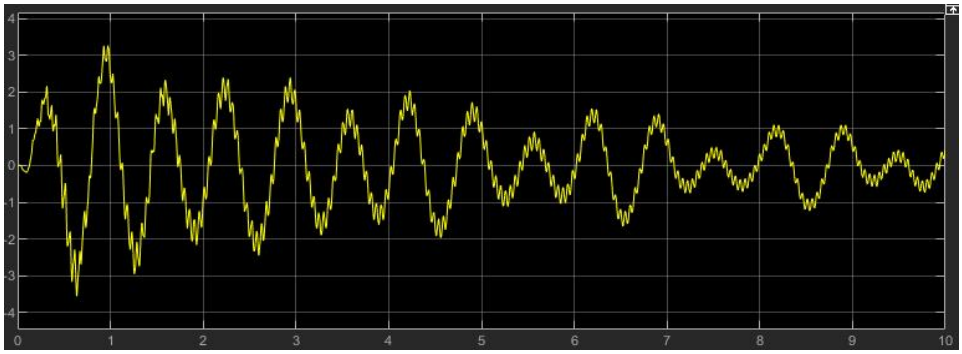


*Figure 24- Hip acceleration in the forward direction (y-axis) in this case. The P2P value for the acceleration is calculated as 6.908 m/s$^2$ and STD is 1.105. The velocity is 0.2m/s.*

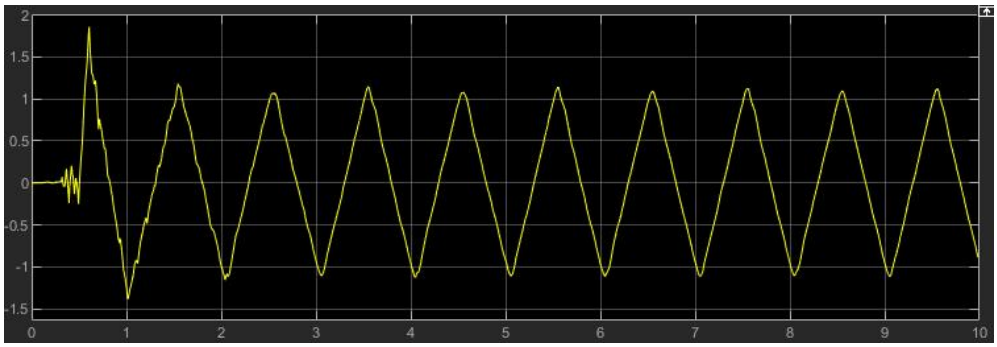


*Figure 25- ankle acceleration in the forward direction (y-axis) in this case. The P2P value for the acceleration is calculated as 3.271 m/s$^2$ and STD is 0.683. the velocity is 0.2m/s.*

| Axes | | $v_1$(0.025 m/s) | | $v_1$(0.05 m/s) | | $v_1$(0.1 m/s) | | $v_1$(0.025 m/s) | |
|---|---|---|---|---|---|---|---|---|---|
| | | Foot | Hip | Foot | Hip | Foot | Hip | Foot | Hip |
| **X** | P2P | 0.398 | 1.223 | 1.110 | 1.561 | 0.397 | 1.708 | 1.599 | 2.765 |
| | STD | 0.025 | 0.125 | 0.025 | 0.132 | 0.0273 | 0.170 | 0.068 | 0.262 |
| **Y** | P2P | 0.631 | 0.970 | 1.049 | 1.915 | 1.528 | 3.654 | 3.271 | 6.908 |
| | STD | 0.086 | 0.158 | 0.171 | 0.314 | 0.334 | 0.608 | 0.683 | 1.105 |
| **Z** | P2P | 0.417 | 0.805 | 0.438 | 2.446 | 0.486 | 3.367 | 1.598 | 4.899 |
| | STD | 0.019 | 0.688 | 0.022 | 0.436 | 0.024 | 0.524 | 0.115 | 0.587 |

*Table 6 - Accelerations during a forward motion in Configuration 2.*

The results in both configuration shows that the number of passive elements, in this case which are springs, increases the amount of oscillations generated in the robotic body. As expected also the oscillations around the hip joint is more as compared to the oscillations noted at the ankle joint.

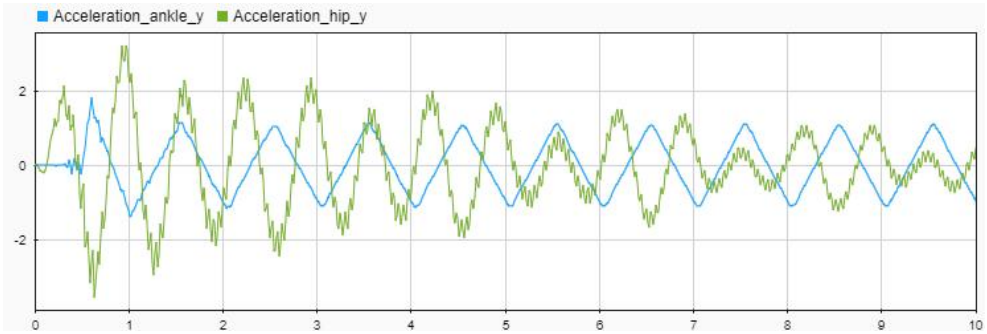


*Figure 26 - the acceleration in y-axis in configuration 2. (Green) shows the acceleration at the hip and (purple) shows the acceleration at the ankle.*

If we look closely at the result shown in the figure and table given above, we can see that the oscillation occurs in acceleration in Hip in the y-axis, during the forward motion, is greater than the ankles' y-axis. The P2P value of acceleration around the hip is 6.908 $m/s^2$ whereas, around ankle it is 3.271 $m/s^2$. The STD at hip is 1.105, which is far more than the one measured around ankle 0.608.

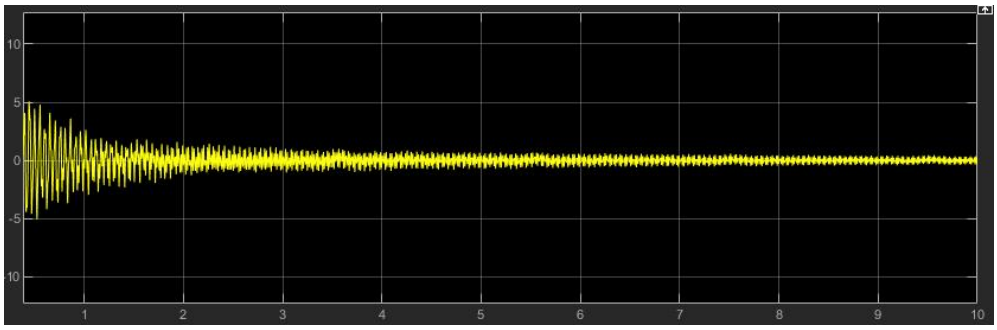


*Figure 27 - the acceleration in z-axis (at the velocity=0.2m/s) around hip joint in configuration 2: three springs in each leg.*

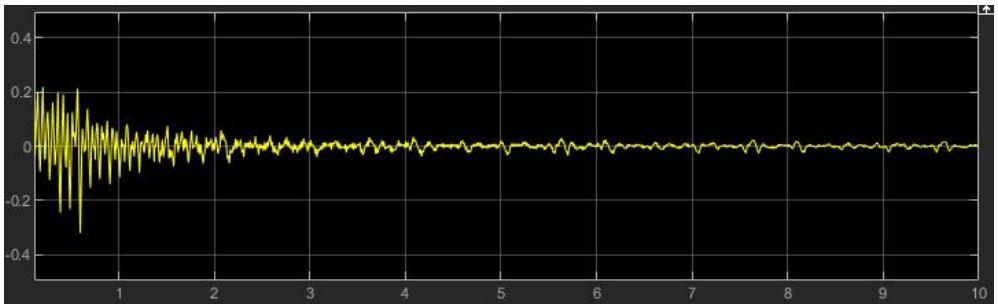


*Figure 28 - acceleration in z-axis (at the velocity=0.2m/s) around ankle joint in configuration 2: three springs in each leg.*

looking at Figures above, it can be seen how the acceleration at z-axis (ankle) has oscillations absolute minimum and maximum value respectively of -0.321 $m/s^2$ and 0.0219 $m/s^2$; the acceleration at z-axis (hip) has oscillations with absolute minimum and maximum value respectively of -2.697 $m/s^2$ and 1.916 $m/s^2$.

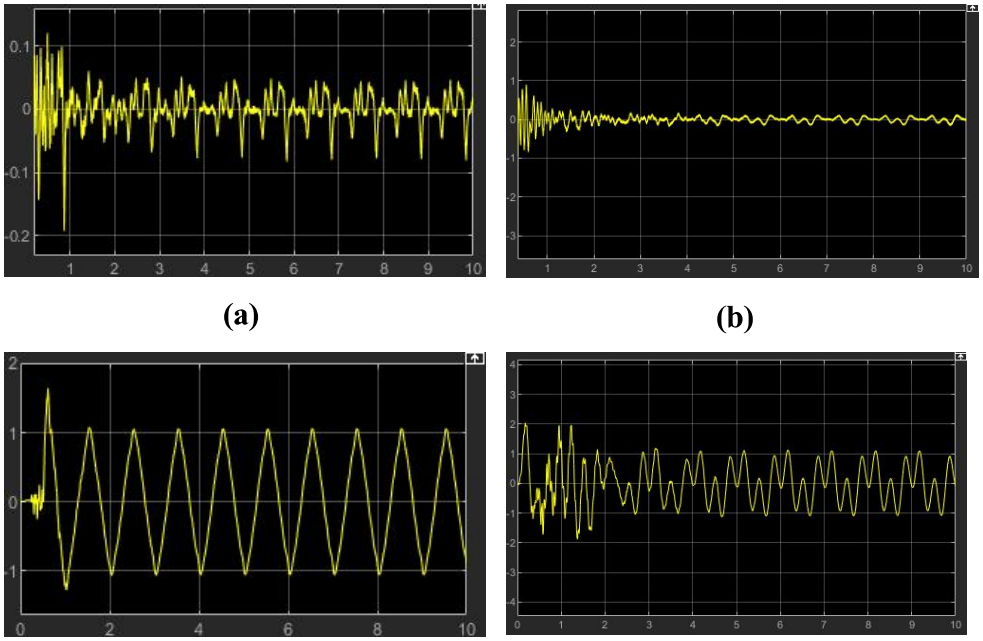

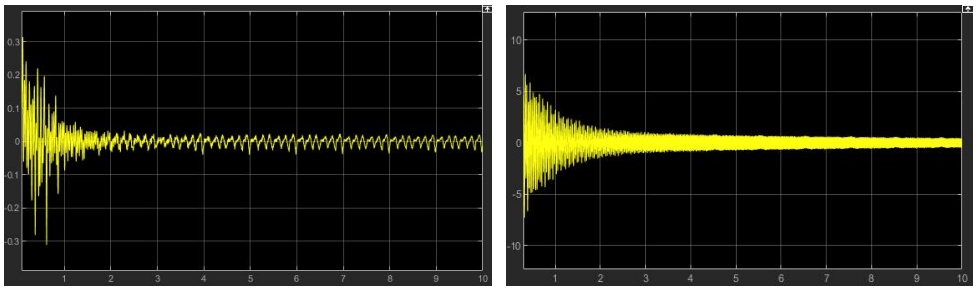

**(e)** (f)

*Figure 29 - represents the values of acceleration in configuration 1: with 2 springs in each leg. The velocity is 0.2 m/s. figure a, c and e represent the acceleration at ankle at x, y and z axis respectively. Whereas b, d and f represent the acceleration around hip at x, y and z axis respectively*

Figures 29 and 30 shows the detailed result in both configurations reconfirm these aspects, related to the behavior of the flexible structure of the robot, showing the difference of the output signals of the accelerometers, and therefore the relative acceleration of the hip with respect of the foot, during a motion with the minimum *velocity = 0.2 m/s*.

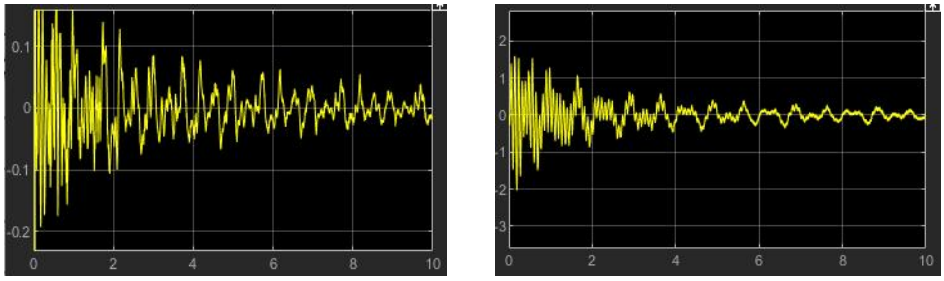

**(a)** **(b)**

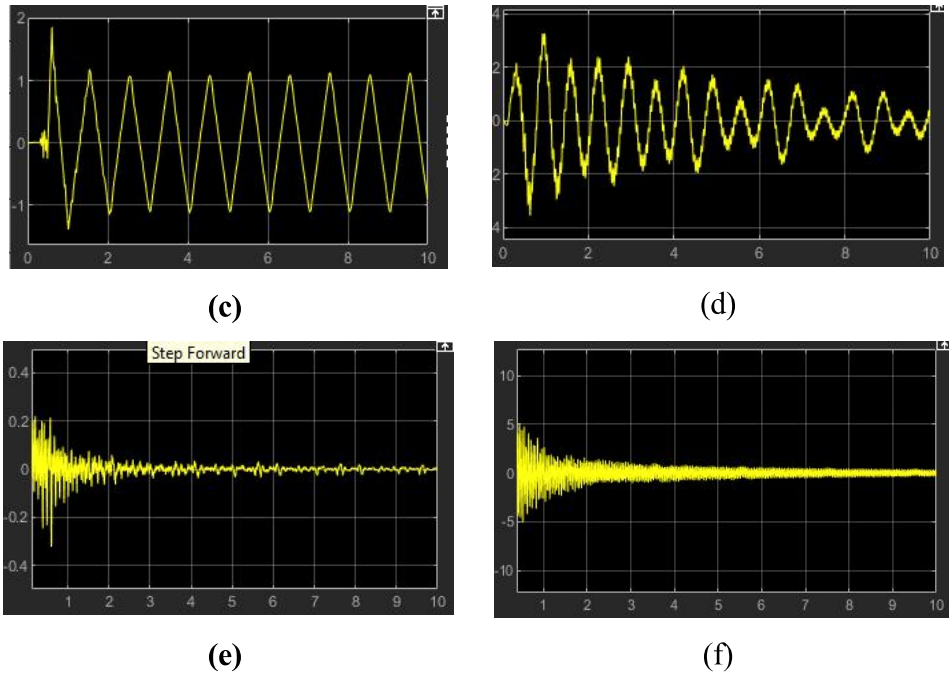


*Figure 30 - represents the values of acceleration in configuration 2: with 3 springs in each leg. The velocity is 0.2 m/s. figure a, c and e represent the acceleration at ankle at x, y and z axis respectively. Whereas b, d and f represent the acceleration around hip at x, y and z axis respectively*

The figures (a, c and e) represents the acceleration in x, y and z axis respectively whereas b, d and f represent the acceleration around hip at x, y and z axis respectively and it can be seen clearly and also to match the results from the table that P2P value and STD value in the ankle with respect to hip is much less. The similar result can be observed by comparing the P2P and STD values of the acceleration between the two configurations.

### 4.3 Comparison with ROLLO prototype

The results of this research is briefly compared with the outcome of the ROLLO prototype created in BrainHuro project [54] and shown in the following figures.

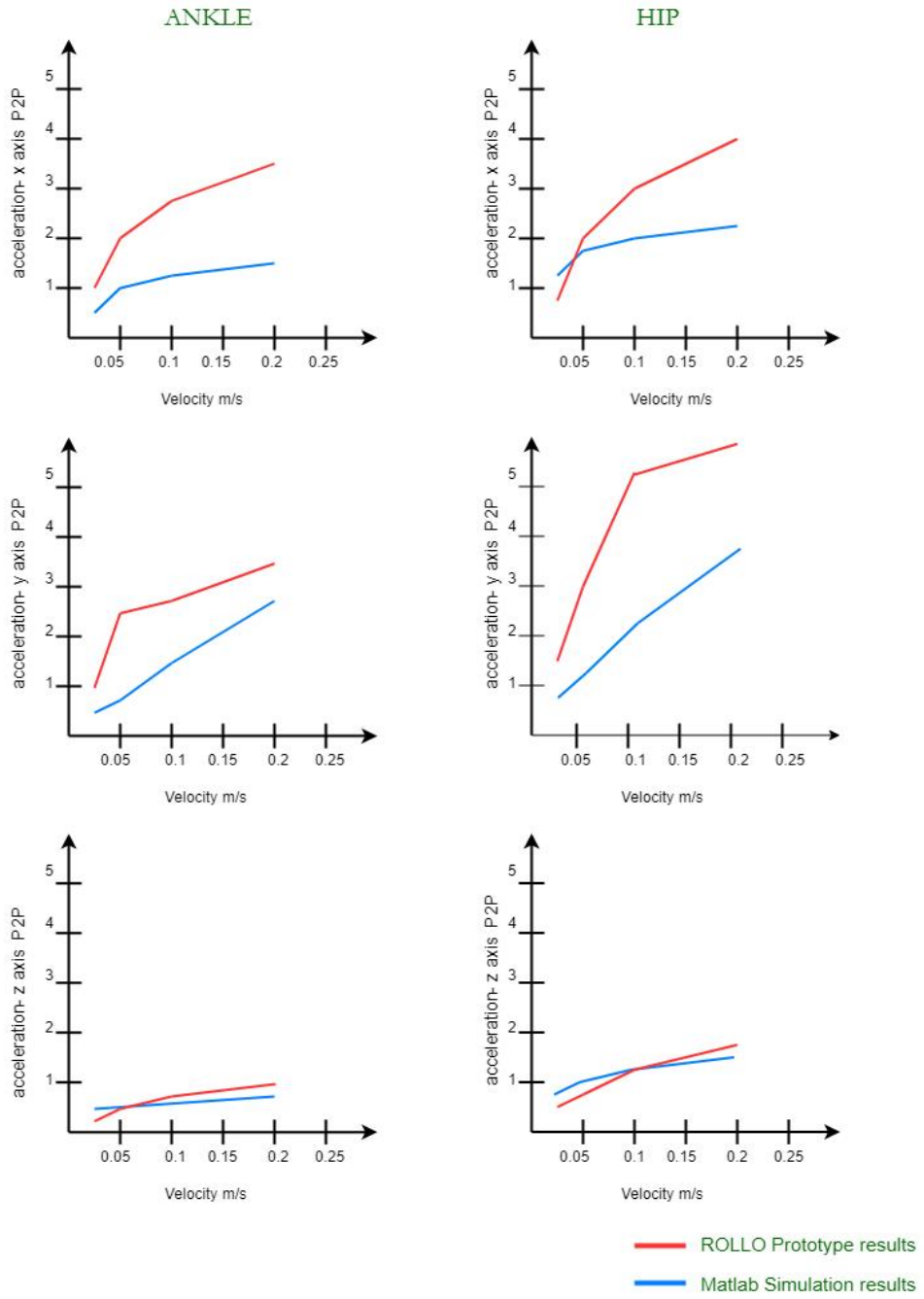


*Figure 31 – Shows the difference in the acceleration (P2P) results between ROLLO prototype and Simulation done in Matlab. The velocity is 0.2 m/s and robot is in configuration 1. (2 springs in each leg)*

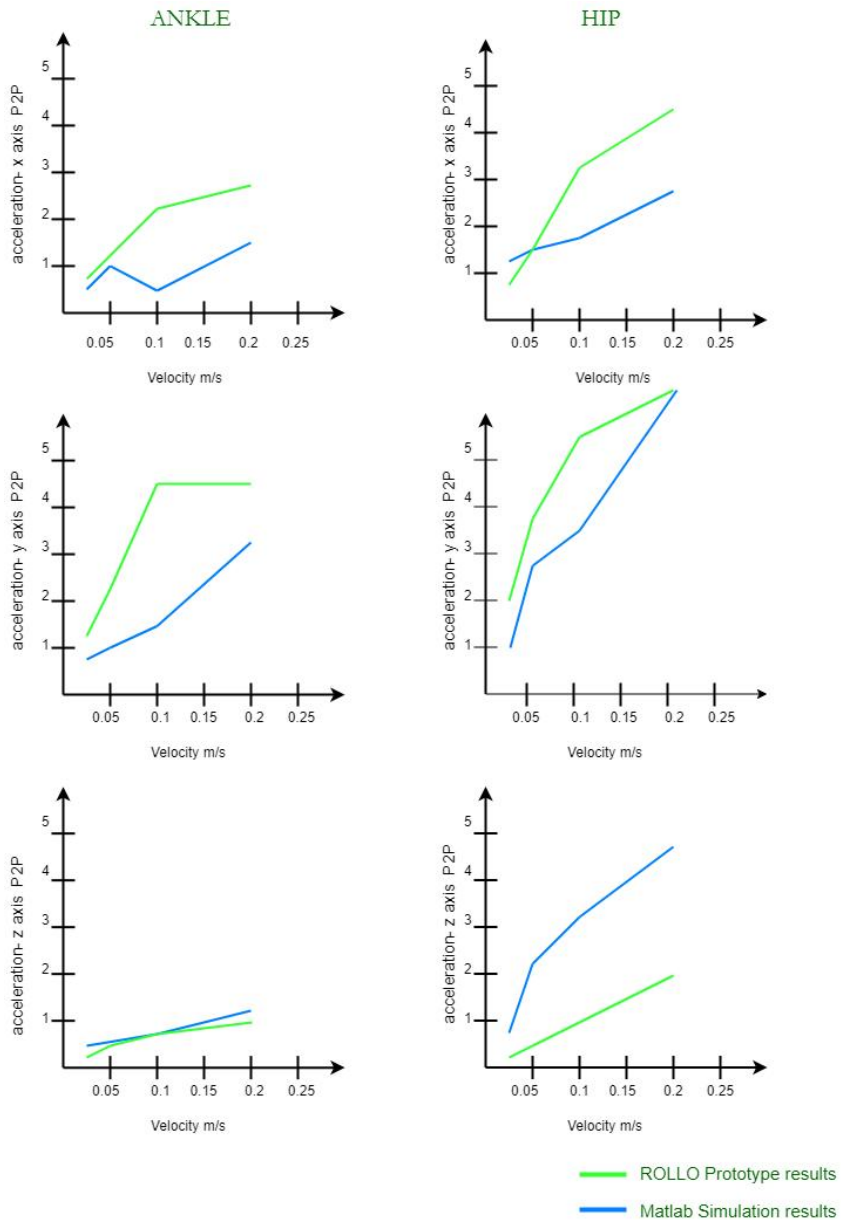


*Figure 32 – Shows the difference in the acceleration (P2P) results between ROLLO prototype and Simulation done in Matlab. The velocity is 0.2 m/s and robot is in configuration 1. (2 springs in each leg)*

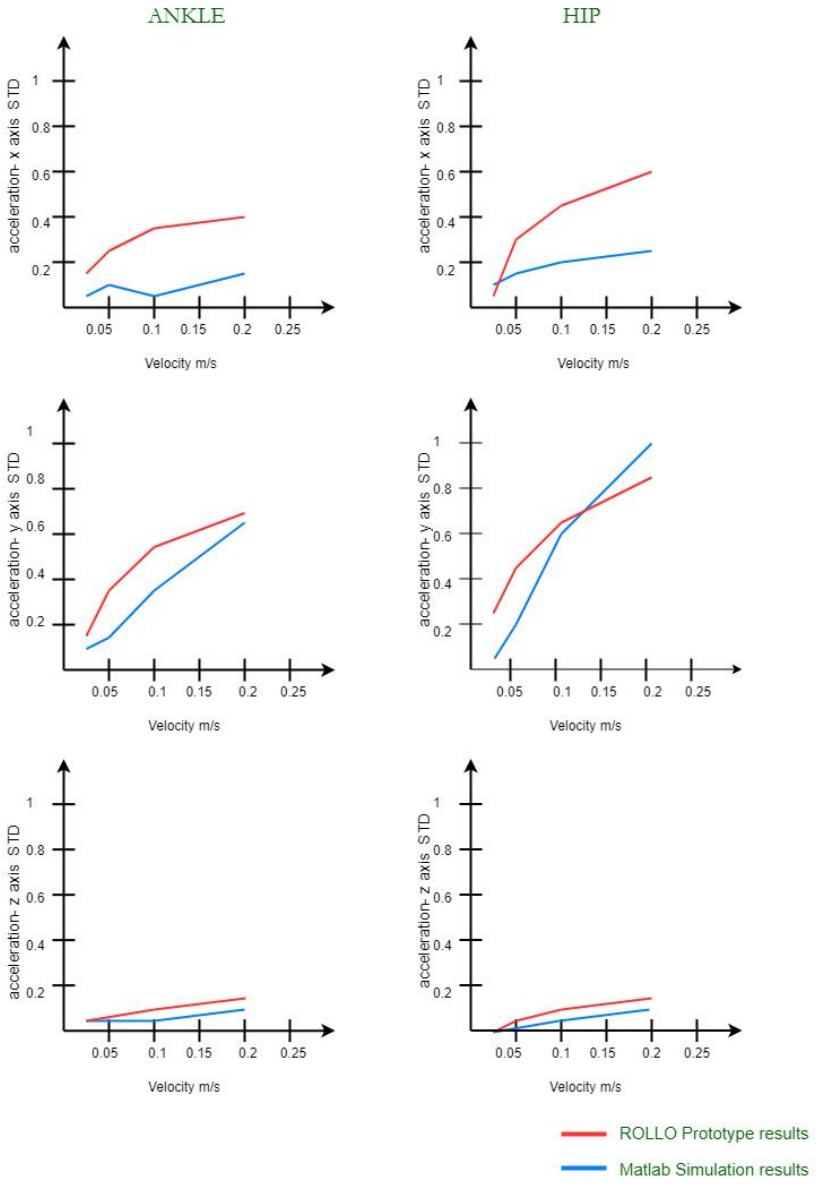


*Figure 33 - Shows the difference in the acceleration (STD) results between ROLLO prototype and Simulation done in Matlab. The velocity is 0.2 m/s and robot is in configuration 1. (2 springs in each leg)*

The data above definitely reflects the improvement (except some irregularities) in the results of ROLLO robot, by working on the better control technologies

and finding an optimized motion profiles there is always a room to improve the desired result and make the system more efficient. The result is obtained by introducing a different layer of control and filtration. The detailed result of this is discussed in the section 4.5.

### 4.4 Torque w.r.t stiffness

As discussed above about the efficiency of the system as compared to the one using rigid link. Despite of using more actuation force around all the joints, even the torque required to derive even a single link is much higher in case of rigid link than the flexible link.

The test has been carried out with the different stiffness of the links and torque required by a motor to obtain a same motion profile is much different.

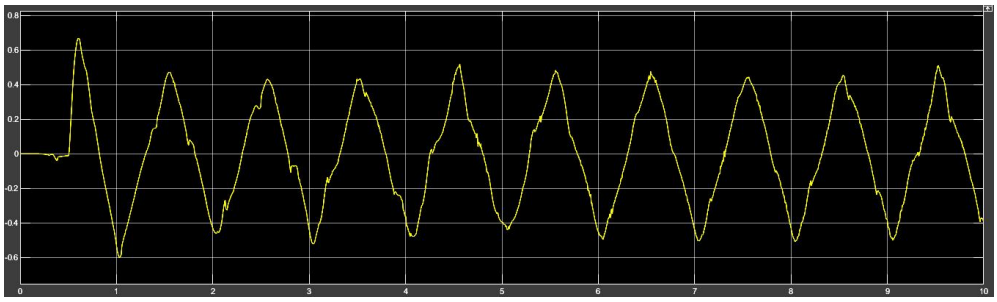


*Figure 34 - the torque required by a motor in configuration one to perform human like walking at velocity=0.2 m/s. The stiffness of the springs is 1.40 daN/mm and 18Nmm/deg.*

On the above mentioned configuration of the spring's stiffness the P2P value of the torque produced by motor on velocity=0.2 *m/s* is 1.268. while the robot with the same configurations and motion profile but with the different value of the spring's stiffness requires much more torque from the motors. The P2P value of the torque produced by motor with the spring stiffness of 70.4 daN/mm at velocity=0.2 *m/s* is 10.737.

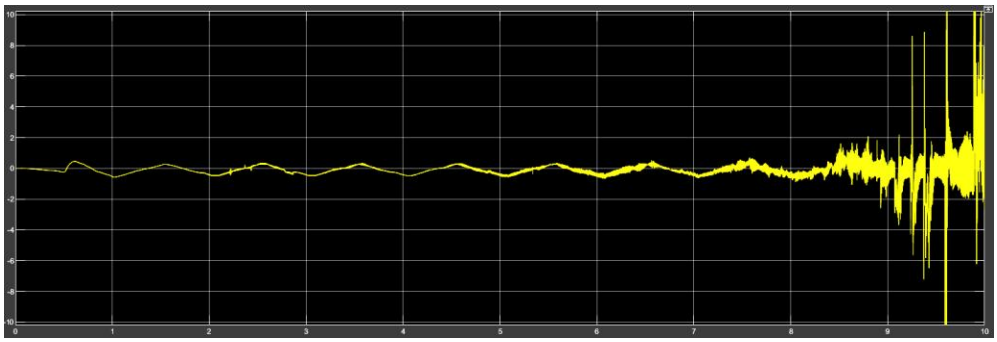

*Figure 35 - the torque required by a motor in configuration one to perform human like walking at velocity=0.2 m/s. The stiffness of the springs is 70.4 daN/mm and 20Nmm/deg.*

It is clearly evident from the graphs above that the to present the same motion at the same velocity the torque can vary with the variation in the stiffness of the body. Stiffer the body is; more actuation force/torque would be required.

### 4.5 Controller Results

The close examination in the figures below shows that the derivatives or the slopes of the torque before smoothing the input trajectory is much steeper as compared to the smoothed ones.

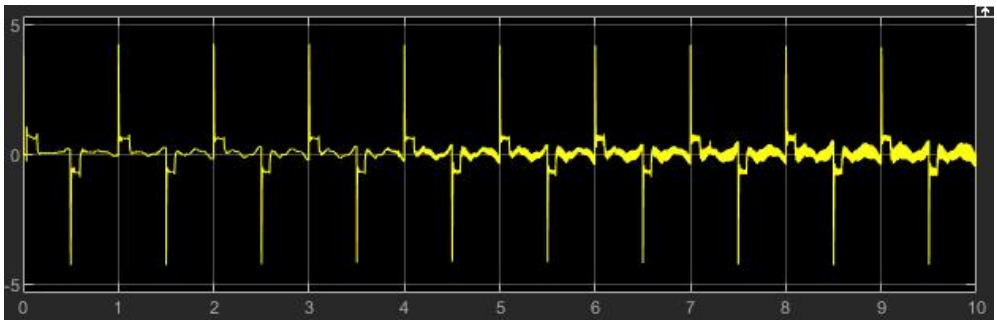


*Figure 36 – Torque produced by wheels to produce the desire motion without smoothing the motion profile.*

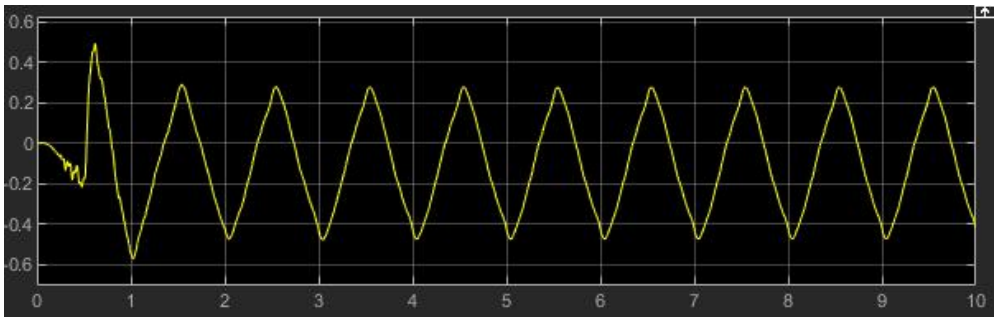


*Figure 37 - Torque produced by wheels to produce the desire motion with smooth motion profile and the implementation of control strategies.*

By smoothing our curves and introduction of control, we make sure that our required torque doesn't change very quickly thus preventing the hard stop. The comparison of accelerations P2P and STD values, before and after implementation of control is presented in the table below.

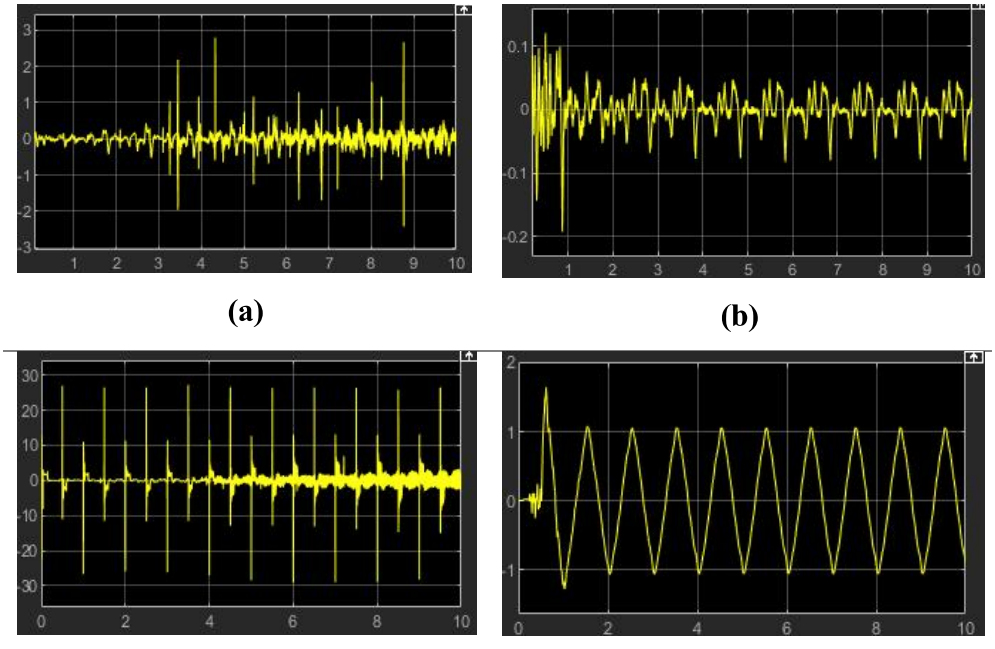


**(a)** **(b)**

**(c)** (d)

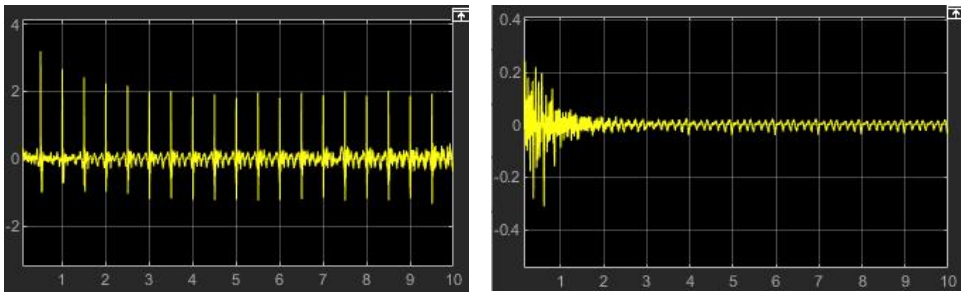

**(e)** (f)

*Figure 38 - Acceleration in x, y and z axis during the forward motion in the configuration 1 at velocity= 0.2 m/s before the implementation of PID controller and filtration (a, c, e) and figure (b, d, f) shows the acceleration in x, y and z respectively after the implementation of the control strategies.*

Without the suitable control, ROLLO robot is still able to perform the biped locomotion but with far less efficiency and unnatural gait. As shown in , The table below contains the detailed comparison of parameters such as acceleration

| Parameters | | Before the control | After the control |
|---|---|---|---|
| **Torque produced by motor** | | 8.537 | 1.062 |
| **Acceleration x-axis (ankle)** | P2P | 3.960 | 1.438 |
| | STD | 0.703 | 0.115 |
| **Acceleration y-axis (ankle)** | P2P | 5.629 | 2.901 |
| | STD | 2.325 | 0.667 |
| **Acceleration z-axis (ankle)** | P2P | 1.670 | 0.529 |
| | STD | 0.316 | 0.1297 |

*Table 7 – depicts the comparison of the system performing the alternating biped locomotion at velocity=0.2 m/s at configuration 1 , with and without control*

at ankle joint and torque while performing a forward alternative leg motion on velocity=0.2 m/s in configuration 1 (2 springs in each leg).

### 4.6 Summary and future work

Above mentioned research is based on the simulation of creative design and simulation inspired by ROLLO robot (developed in BrainHuRo project) [54], The main focus of this project is to produce a humanoid robot which is able to move flexibly in the human space, without consuming an extravagant amount of energy. Which is less complex to control but at the same time perform the tasks of humanoid robots by maintaining the lower impact on the environment.

This novel approach is the result of the extensive understanding of traditional ZMP based control used in the traditional humanoid and provide us with a bypass to this approach. The approach experimentally suggest that it is not necessary to have a complex structure with excessive number of DOFs, the same functions can be provided by comparatively less complex structure. It is done by introducing wheels on the feet and replacing the rigid links in the legs with the flexible link. By exploiting the torsional and flexural behaviors of the flexible links, the presence of actuated joints in the knee and hip is avoided, replacing them with the passive joints instead. This allowed the robot to perform an alternating leg human like motion by using only two motors. There are 2 free wheels on each leg, which allows the robot to maintain the standing position without any actuation. Unconventional use of the cylindrical helical springs would improve the power consumption of the robot as well as they would pose much safer in the domestic environment.

The modelling and simulation of the ROLLO robot to create a dynamic simulation of the human like movement has been realized using 2 different software Solid works and MATLAB. The 3D-modelling of the Robot is done in solid works (except springs). The torsional and flexural behavior of the springs and the control of the ROLLO robot in the world environment was performed in MATLAB. The various level of controls has been utilized for the stable gait. The low level of control was developed to smoothen the input trajectory to avoid the hard stop thus reducing the oscillations. Filtration and PID controller was also used, they have been tuned by considering the system into feedback loop and different kind of disturbances were added to set the controller parameters and get the nominal steady state response. The tradeoff between balance, energy consumption and the oscillations have been performed in the different level of controls. The different results are obtained on 4 distinct velocities and 2 different configurations of the leg (one with 2 springs in each leg the other one is 3 springs in each leg) while performing the forward motion and rotation (clockwise anticlockwise) on the planar surface.

This simulation of the ROLLO in MATLAB is the initial point of a broad spectrum of other possible future works: from the control structure completion and whole-body control application, to deep learning and reinforcement learning for human locomotion, from testing in the flat domestic environment and testing in the rough terrain with obstacle and certainly the transition from simulation to practice on the real platform such as ROLLO developed at BrainHuRo. Exploiting the vast availability of different functions in MATLAB would allow the researchers to get the interesting results.

# BIBLIOGRAPHY


1. G. G. Muscolo, C. T. Recchiuto and R. Molfino (2015). Dynamic balance optimization in biped robots: Physical modeling, implementation and tests using an innovative formula. Robotica, 33, pp 2083-2099 doi:10.1017/S0263574714001301
2. G. G. Muscolo, K. Hashimoto, A. Takanishi and P. Dario (2013). A Comparison between Two Force-Position Controllers with Gravity Compensation Simulated on a Humanoid Arm. Journal of Robotics, volume 2013, Article ID 256364, 14 pages
3. G. G. Muscolo, C. T. Recchiuto, Flexible Structure and Wheeled Feet to Simplify Biped Locomotion of Humanoid Robots, 22 December 2016, in International Journal of Humanoid Robotics Vol. 14, No. 1, World Scientific Publishing Company, 2017
4. Diego Torricelli et al 2016, Human-like compliant locomotion: state of the art of robotic implementations, Bioinspir. Biomim. **11** 051002
5. P. Fedele, P. Federighi, R. Molfino, G. G. Muscolo, C.T Recchiuto, A. Rufa, 2014, High energy efficiency biped robot controlled by the human brain for people with ALS disease. Proceedings of the Mediterranean Electrotechnical Conference – MELECON. Pages 386-392
6. G. G. Muscolo, C. T. Recchiuto and R. Molfino (2014). Vision and locomotion control systems on a bio-inspired humanoid robot. Proceedings of the Mediterranean Electrotechnical Conference – MELECON. Pages 380-385

7. McGeer T. Passive dynamic walking. Int J Robot Res. 1990; 9: 62–82.
8. M. H. Raibert, H. B. Brown, M. Chepponis, E. Hastings, J. Koechling, K. N. Murphy, S. S. Murthy, A. J. Stentz Dynamically Stable Legged Locomotion. 1983 The Robotics Institute and Department of Computer Science Ca rnegie-Mellon University Pittsburgh, PA. 15213
9. Kuo AD. Choosing Your Steps Carefully: Trade-offs between economy and versatility in dynamic walking bipedal robots. IEEE Robot Autom Mag. 2007; 14: 18–29. https://doi.org/10.1109/MRA.2007.380653
10. Wisse M. Three additions to passive dynamic walking: actuation, an upper body, and 3d stability. Int J Humanoid Robot. 2005; 2: 459–478.
11. Kuo AD. Stabilization of lateral motion in passive dynamic walking. Intl J Robot Res. 1999; 18: 917–930.
12. N. Shafii, A. Abdolmaleki, R. Ferreira, N. Lau and L. P. Reis. Towards Fast Walking based on ZMP Control and Central Pattern Generator. 2013
13. H.- Lim, Y. Kaneshima and A. Takanishi,"Online Walking Pattern Generation for Biped Humanoid Robot with Trunk", Proceedings of the 2002 IEEE International Conference on Robotics & Automation, Washington, DC (May 2002).
14. S. J. Kwon and Y. Oh, "Estimation of the Center of Mass of Humanoid Robot", Proceedings of the International Conference on Control, Automation and Systems 2007, COEX, Seoul, Korea (Oct. 17–20, 2007)

15. Ito, Satoshi & Nishio, Shingo & Fukumoto, Yuuki & Matsushita, Kojiro & Sasaki, Minoru. (2017). Gravity Compensation and Feedback of Ground Reaction Forces for Biped Balance Control. Applied Bionics and Biomechanics. 2017. 10.1155/2017/5980275.
16. B. Vanderborght, “Dynamic Stabilisation of the Biped Lucy Powered by Actuators with Controllable Stiffness”, Star, Springer tracts in advanced robotics, 63 (2010).
17. Wang, W., Fu, X., Li, Y., & Yun, C. (2018). Design and implementation of a variable stiffness actuator based on flexible gear rack mechanism. Robotica, 36(3), 448-462. doi:10.1017/S0263574717000492
18. R. Ranjan, P.K. Upadhyay, A. Kumar and P. Dhyani (2012). Theoretical and Experimental Modeling of Air Muscle. International Journal of Emerging Technology and Advanced Engineering. Volume2, issue 4.
19. L. Zollo, B. Siciliano, A. De Luca, and E. Guglielmelli, “PD control with online gravity compensation for robots with flexible links,” in Proceedings of the European Control Conference, Kos, Greece, July 2007
20. Vadakkepat, Prahlad & Goswami, Dip. (2008). BIPED LOCOMOTION: STABILITY, ANALYSIS AND CONTROL. International Journal on Smart Sensing and Intelligent Systems. 1. 10.21307/ijssis-2017-286.
21. C. Chevallereau, E. Westervelt and J. Grizzle. Asymptotically Stable Running for a Five-Link, Four-Actuator, Planar Bipedal Robot. International Journal of Robotics Research, SAGE Publications, 2005, 24 (6), pp.431-464.

22. Piiroinen, P., Dankowicz, H., & Nordmark, A. (2001). On a normal-form analysis for a class of passive bipedal walkers. International Journal of Bifurcation and Chaos, 11(9), 2411–2425.
23. Garcia, E., Estremera, J., & Gonzales de Santos, P. (2002). A comparative study of stability margins for walking machines. Robotica, 20, 595–606
24. Hemami, H., Zheng, Y. F., & Hines, M. J. (1982). Initiation of walk and tiptoe of a planar nine link biped. Mathematical Biosciences, 61, 163–189
25. J. Y. Hung, W. Gao and J. C. Hung, "Variable structure control: a survey," in IEEE Transactions on Industrial Electronics, vol. 40, no. 1, pp. 2-22, Feb. 1993. doi: 10.1109/41.184817
26. F. N. Al-Shuka, Hayder & Corves, Burkhard & Zhu, Wen-Hong. (2013). On the Dynamic Optimization of Biped Robot. Lecture Notes on Software Engineering. 01. 237-243. 10.7763/LNSE.2013.V1.52.
27. Fujiwara, K., Kanehiro, F., Kajita, S., Kaneko, K., Yokoi, K., & Hirukawa, H. (2002). UKEMI: Falling motion control to minimize damage to biped humanoid robot. Proceedings of the 2002 IEEE/RSJ international conference on intelligent robots and systems, EPFL, Lausanne, Switzerland (pp. 2521–2526).
28. Wieber, P. B. (2002). On the stabilityof walking systems. Third IARP international workshop on humanoid and human friendly robotics, December 11–12, Tsukuba Research Center, Ibaraki, Japan.
29. Hurmuzlu, Yildirim & Génot, Frank & Brogliato, Bernard. (2004). Modeling, Stability and Control of Biped Robots A General Framework. Automatica. 40. 1647-1664.10.1016/j.automatica.2004.01.031.

30. K. Endo, T. Maeno and H. Kitano, "Co-evolution of morphology and walking pattern of biped humanoid robot using evolutionary computation. Consideration of characteristic of the servomotors," IEEE/RSJ International Conference on Intelligent Robots and Systems, Lausanne, Switzerland, 2002, pp. 2678-2683 vol.3. doi: 10.1109/IRDS.2002.1041674
31. M. Inaba, T. Igarashi, S. Kagami and H. Inoue, "A 35 DOF humanoid that can coordinate arms and legs in standing up, reaching and grasping an object," Proceedings of IEEE/RSJ International Conference on Intelligent Robots and Systems. IROS '96, Osaka, Japan, 1996, pp. 29-36 vol.1.
doi: 10.1109/IROS.1996.570622
32. K. Kaneko et al., "Design of advanced leg module for humanoid robotics project of METI," Proceedings 2002 IEEE International Conference on Robotics and Automation (Cat. No.02CH37292), Washington, DC, USA, 2002, pp. 38-45 vol.1.
doi: 10.1109/ROBOT.2002.1013336
33. Yin, Kangkang & Loken, Kevin & van de Panne, Michiel. (2007). SIMBICON: simple biped locomotion control. ACM Trans. Graph. 26. 105. 10.1145/1275808.1276509.
34. Nakanishi, Jun & Morimoto, Jun & Endo, G & Cheng, Gordon & Schaal, Stefan & Kawato, Mitsuo. (2003). Learning from Demonstration and Adaptation of Biped Locomotion with Dynamical Movement Primitives. Robotics and Autonomous Systems - RaS. 2004. 10.1299/jsmermd.2004.32_2.
35. F. Iida, Y. Minekawa, J. Rummel, A. Seyfarth, Toward a human-like biped robot with compliant legs, Robotics and Autonomous Systems,

Volume 57, Issue 2,2009, Pages 139-144, ISSN 0921-8890, https://doi.org/10.1016/j.robot.2007.12.001.

36. Wu, Jia-chi & Popovic, Zoran. (2010). Terrain-adaptive bipedal locomotion control. ACM Transactions on Graphics. 29. 1. 10.1145/1833351.1778809.
37. Zhao, Ye & Fernández Rodríguez, Benito & Sentis, Luis. (2016). Robust Phase-Space Planning for Agile Legged Locomotion over Various Terrain Topologies. 10.15607/RSS.2016.XII.010.
38. J. H. Park and Y. K. Rhee, "ZMP trajectory generation for reduced trunk motions of biped robots," Proceedings. 1998 IEEE/RSJ International Conference on Intelligent Robots and Systems. Innovations in Theory, Practice and Applications (Cat. No.98CH36190), Victoria, BC, Canada, 1998, pp. 90-95 vol.1. doi: 10.1109/IROS.1998.724602
39. VUNDAVILLI, P.R. & PRATIHAR, D.K. Sadhana (2011) Balanced gait generations of a two-legged robot on sloping surface 36: 525. https://doi.org/10.1007/s12046-011-0031-7
40. P. Tomei, “A simple PD controller for robots with elastic joints,” IEEE Trans. Autom. Control, vol. 36, no. 10, pp. 1208–1213, Oct 1991.
41. A. D. Luca, B. Siciliano, and L. Zollo, “PD control with on-line gravity compensation for robots with elastic joints: Theory and experiments,” Automatica, vol. 41, no. 10, pp. 1809 – 1819, 2005.
42. Tsagarakis, Nikos & Li, Zhibin & Saglia, J.A. & G. Caldwell, Darwin. (2011). The design of the lower body of the compliant humanoid robot “cCub”. 2035 - 2040. 10.1109/ICRA.2011.5980130.
43. M. Laffranchi, N. G. Tsagarakis and D. G. Caldwell, “Antagonistic and Series Elastic Actuators: a Comparative Analysis on the Energy

Consumption,” in International Conference on Intelligent Robots and Systems, St. Louis, 2009.

44. A. Jafari, N. G. Tsagarakis, and D. G. Caldwell, "Exploiting Natural Dynamics for Energy Minimization using an Actuator with Adjustable Stiffness (AwAS)," presented at the International Conference on Robotics and Automation, Shanghai, China, 2011.
45. A. De Luca and W. Book, "Robots with Flexible Elements," in Handbook of Robotics, S. K. Editors, Ed., ed: Springer, 2008.
46. T. E. Milner and C. Cloutier, "Damping of the wrist joint during voluntary movement," Experimental Brain Research, vol. 122, pp. 309- 317, 1998.
47. Laffranchi, Matteo & Chen, Lisha & Tsagarakis, Nikos & G. Caldwell, Darwin. (2012). The role of physical damping in compliant actuation systems. Proceedings of the ... IEEE/RSJ International Conference on Intelligent Robots and Systems. IEEE/RSJ International Conference on Intelligent Robots and Systems. 3079-3085. 10.1109/IROS.2012.6385883.
48. P. Fedele, P. Federighi, R. Molfino, G. G. Muscolo, C. T. Recchiuto and A. Rufa, High energy efficiency biped robots controlled by the human brain for people with ALS disease,in 17th IEEE Mediterranean Electro technical Conference (MELECON 2014), 13–16 April 2014 (Beirut, Lebanon, 2014).
49. G. G. Muscolo, C. T. Recchiuto, K. Hashimoto, C. Laschi, P. Dario and A. Takanishi, a method for the calculation of the effective center of mass of humanoid robots, in 11th IEEE–RAS Int. Conf. on Humanoid Robots (Humanoids 2011), 26th–28th October 2011 (Bled-Slovenia, 2011).

50. G. G. Muscolo, C. T. Recchiuto and R. Mol¯no, Dynamic balance optimization in biped robots: Physical modeling, implementation and tests using an innovative formula, Robotica 33(10) (2015) 2083–2099.
51. G. G. Muscolo, K. Hashimoto, A. Takanishi and P. Dario, A comparison between two force-position controllers with gravity compensation simulated on a humanoid arm, J. Robotics 2013 (2013) 14.
52. G. G. Muscolo, C. T. Recchiuto and R. Mol¯no, Vision and locomotion control systems in a bioinspired humanoid robot, in 17th IEEE Mediterranean Electrotechnical Conference (MELECON 2014), 13–16 April 2014 (Beirut, Lebanon, 2014).
53. G. G. Muscolo and C. T. Recchiuto, Propelled bipedal robotic apparatus. Property of the Humanots.r.l.. Patent Pending. 102015000049099 (2015).
54. Humanot Company, available at http://www.humanot.it
55. Liquidweb Company, available at http://www.liquidweb.it.
56. G. G. Muscolo, C. T. Recchiuto, K. Hashimoto, C. Laschi, P. Dario and A. Takanishi, A method for the calculation of the effective center of mass of humanoid robots, in 11th IEEE–RAS Int. Conf. on Humanoid Robots (Humanoids 2011), 26th–28th October 2011 (Bled-Slovenia, 2011).
57. G. G. Muscolo, C. T. Recchiuto and R. Molfino, Dynamic balance optimization in biped robots: Physical modeling, implementation and tests using an innovative formula, Robotica 33(10) (2015) 2083–2099
58. G. G. Muscolo and C. T. Recchiuto, T.P.T.: A novel taekwondo personal trainer robot, Robot. Auton. Syst. 83 (2016) 150–157, available at http://dx.doi.org/10.1016/j.robot. 2016.05.009.

59. R. Molfino, G. G. Muscolo, D. Puig, C. T. Recchiuto, A. Solanas and A. M. Williams, An Embodied-Simplexity Approach to Design Humanoid Robots Bioinspired by Taekwondo Athletes, in TAROS 2013, LNAI 8069, eds. A. Natraj et al. (Springer-Verlag, Berlin, Heidelberg, 2014), pp. 1–2, Doi: 10.1007/978-3-662-43645-5 34.
60. L. Della Pietra, The Dynamic Coupling of Torsional and Flexural Strains in Cylindrical Helical Springs (Meccanica, Springer, New York, 1976)
61. A. M. Yu and Y. Hao, Free vibration analysis of cylindrical helical springs with noncircular cross-sections, J. Sound Vib. 330 (2011) 2628–2639.
62. C. J. Yang, W. H. Zhang, G. X. Ren and X. Y. Liu, Modeling and dynamics analysis of helical spring under compression using a curved beam element with consideration on contact between its coils, Meccanica 49 (2014) 907–917, Doi: 10.1007/s11012-013-9837-1
63. W. H. Wittrick, On elastic wave propagation in helical springs, Int. J. Mech. Sci. 8(1) (1966) 25–47
64. G. A. Bekey, "Springer Handbook of Robotics (B. Siciliano and O. Khatib; 2008) [Book Review]," in IEEE Robotics & Automation Magazine, vol. 15, no. 3, pp. 110-110, September 2008. doi:10.1109/MRA.2008.928399
65. Mark W. Spong. 1989. Robot Dynamics and Control (1st ed.). John Wiley & Sons, Inc., New York, NY, USA.
66. [Mu and Wu, 2003] Mu, X. and Wu, Q. (2003). A complete dynamic model of fivelink bipedal walking. Proceedings of the American Control Conference. [CDROM, 2007, literature/modeling/complete dynamic model.pdf]

67. L. Bascetta and P. Rocco. Modelling flexible manipulators with motors at the joints. Mathematical and Computer Modelling of Dynamical Systems, 8(2): 157–183, 2002.
68. Otten E. Inverse and forward dynamics: models of multi-body systems. Philos Trans R Soc Lond B Biol Sci. 2003;358(1437):1493–1500. doi:10.1098/rstb.2003.1354
69. K. Yamane and Y. Nakamura. Dynamics filter – concept and implementation of online motion generator for human figures. In Proceedings of the IEEE International Conference on Robotics and Automation, pages 688–694, San Francisco, CA, 2000.
70. Mason, M. T. and Salisbury Jr, J. K. (1985). Robot hands and the mechanics of manipulation